© 2017. Published by The Company of Biologists Ltd | Development (2017) 144, 3674-3685 doi:10.1242/dev.144113

KDM3A-mediated demethylation of histone H3 lysine 9 facilitates the chromatin binding of Neurog2 during neurogenesis

Hao Lin[1,*], Xuechen Zhu[1,*], Geng Chen[1], Lei Song[1], Li Gao[1], Aftab A. Khand[1], Ying Chen[2], Gufa Lin[2,‡] and Qinghua Tao[1,‡]

ABSTRACT

Neurog2 is a crucial regulator of neuronal fate specification and differentiation *in vivo* and *in vitro*. However, it remains unclear how Neurog2 transactivates neuronal genes that are silenced by repressive chromatin. Here, we provide evidence that the histone H3 lysine 9 demethylase KDM3A facilitates the *Xenopus* Neurog2 (formerly known as Xngnr1) chromatin accessibility during neuronal transcription. Loss-of-function analyses reveal that KDM3A is not required for the transition of naive ectoderm to neural progenitor cells but is essential for primary neuron formation. ChIP series followed by qPCR analyses reveal that Neurog2 promotes the removal of the repressive H3K9me2 marks and addition of active histone marks, including H3K27ac and H3K4me3, at the NeuroD1 and Tubb2b promoters; this activity depends on the presence of KDM3A because Neurog2, via its C-terminal domain, interacts with KDM3A. Interestingly, KDM3A is dispensable for the neuronal transcription initiated by Ascl1, a proneural factor related to neurogenin in the bHLH family. In summary, our findings uncover a crucial role for histone H3K9 demethylation during Neurog2-mediated neuronal transcription and help in the understanding of the different activities of Neurog2 and Ascl1 in initiating neuronal development.

KEY WORDS: Neurog2, KDM3A, H3K9me2, Neurogenesis, Histone demethylation, Chromatin accessibility

INTRODUCTION

Neurogenesis is a complex process through which a variety of neurons are generated to populate the central and peripheral nervous systems. Extensive studies in recent decades have revealed that proneural factors in the bHLH family are evolutionarily conserved regulators of neurogenesis in invertebrates and vertebrates (Bertrand et al., 2002). One of the bHLH factors that plays pivotal roles in neurogenesis is neurogenin 2 (Neurog2). Neurog2, a vertebrate homolog of the *Drosophila atonal* gene, is expressed in various domains of the central and peripheral nervous systems (Simmons et al., 2001; Sommer et al., 1996). Neurog2 is a master regulator of neurogenesis in multiple locations, including the neocortex, retina and spinal cord (Heng et al., 2008; Lee and Pfaff, 2003; Mattar et al., 2008; Mizuguchi et al., 2001; Novitch et al., 2001). A common theme for the function of Neurog2 is that it regulates formation of neuronal precursors and initiates the expression of a panel of genes, including NeuroD1, that are necessary for neuronal commitment (Castro and Guillemot, 2011; Wilkinson et al., 2013). The *Xenopus* proneural gene neurogenin-related 1 (*Xngnr1*) is orthologous to mammalian *Neurog2* and plays a hierarchical role in initiating primary neuron formation through multiple neuronal genes, including *Neurod1* and *Myt1* (Bellefroid et al., 1996; Ma et al., 1996). It is well established that Neurog2, via its basic domain, recognizes its targets through binding the E-box DNA regulatory elements with certain degrees of preference. The HLH domain of Neurog2 has been shown to directly or indirectly associate with multiple nuclear factors, controlling context-dependent functions of Neurog2 during neuronal fate specification and diversification (Castro and Guillemot, 2011; Lee and Pfaff, 2003; Wilkinson et al., 2013). Recently, it has been shown that the phosphorylation state of a conserved serine/threonine residue in the second helical domain regulates DNA-binding activities of Neurog2 and Ascl1 (Quan et al., 2016).

The crucial role of Neurog2 in neuronal development has also been demonstrated in direct neuronal reprogramming of non-neural cells *in vivo* and *in vitro* (Aravantinou-Fatorou et al., 2015; Blanchard et al., 2015; Grande et al., 2013; Liu et al., 2016, 2013; Masserdotti et al., 2015; Thoma et al., 2012). It is therefore of central importance to understand how Neurog2 transactivates its neuronal target genes.

Neuronal specification and differentiation during embryonic development involves multiple steps of cell fate transition, during which histone post-translational modifications (PTMs) are of crucial importance (Maze et al., 2013). The ability of Neurog2 to transdifferentiate terminally differentiated non-neural cells into neurons raises the issue of how Neurog2 reinitiates the expression of neuronal genes that are silenced, at least in part, by repressive histone PTMs (Vierbuchen and Wernig, 2012). Previous studies have indicated that Neurog2 is able to recruit the p300/CBP histone acetyltransferase during neurogenesis in the spinal cord, promoting the deposition of active histone marks at neuronal genes (Koyano-Nakagawa et al., 1999; Lee et al., 2009). Neurog2 has also been shown to cooperate with the Brg1-containing chromatin-remodeling complex during retinal neurogenesis (Seo et al., 2005). These findings highlight the ability of Neurog2 to modulate chromatin states suitable for its target activation. However, it remains unclear whether Neurog2 is able to actively remove repressive histone PTMs.

Both di- and tri-methylated histone H3 lysine 9 (H3K9me2/3) are associated with heterochromatin at pericentromeric and telomeric regions, and repress developmental genes (Black et al., 2012; Greer and Shi, 2012). The methylation state of H3K9 is controlled by two groups of enzymes with antagonistic activities. Of interest, lysine demethylases (KDMs) in the Jmjd1 subfamily, including KDM3A (Jmjd1A/JHDM2A), KDM3B (Jmjd1B/JHDM2B) and KDM3C (Jmjd1C), have been characterized to specifically remove dimethylation of H3K9 (Loh et al., 2007; Yamane et al., 2006).

[1]MOE Key Laboratory of Protein Sciences, Tsinghua University School of Life Sciences, Beijing, China 100084. [2]Tongji University School of Life Sciences and Technology, Shanghai, China 200092.
*These authors contributed equally to this work

‡Authors for correspondence (qhtaolab@tsinghua.edu.cn; lingufa@tongji.edu.cn)

X.Z., 0000-0001-5003-8531; Q.T., 0000-0002-2929-1919

Received 3 September 2016; Accepted 25 August 2017

Development (2017) 144, 3674-3685 doi:10.1242/dev.144113

Genetic studies have uncovered crucial roles for KDM3A in several physiological processes, such as spermatogenesis, sexual determination and glucose metabolism (Cheng et al., 2014; Herzog et al., 2012; Kuroki et al., 2013; Liu et al., 2010; Okada et al., 2007; Tateishi et al., 2009). Multiple lines of evidence indicate that removal of H3K9 dimethylation is involved in neuronal differentiation, in addition to many aspects of cellular function. For example, KDM3C (JMJD1C) has been reported to repress neural differentiation of human embryonic stem cells (Wang et al., 2014a) and is required to sustain the expression of miR-302, a crucial epigenetic regulator of pluripotency and neural differentiation (Wang et al., 2014a). In addition, a novel splice variant of LSD1/KDM1A has been recently found to specifically demethylate H3K9me1/2 (Laurent et al., 2015). Depletion of this LSD1 isoform increases H3K9me2 levels at its target promoters and impairs neuronal differentiation *in vitro* (Laurent et al., 2015). Furthermore, KDM7A and PHF8 (aka KDM7B), both of which can demethylate H3K9me1/2 and inhibit other types of histone methylation, have also been implicated in the neural fate control (Huang et al., 2010a,b; Qi et al., 2010; Tsukada et al., 2010).

Studies using the *Xenopus laevis* model have advanced the understanding of mechanisms underlying neural fate specification and determination. The molecular function of Spemann's organizer in neural induction was first uncovered in *Xenopus* (Hemmati-Brivanlou et al., 1994; Sasai et al., 1994; Smith and Harland, 1992). NeuroD1 was initially demonstrated to be able to convert the *Xenopus* naïve ectoderm into neurons (Lee et al., 1995). In the present study, we have performed loss-of-function studies for the *Xenopus* KDM3A and have found evidence that KDM3A is essential for the chromatin accessibility of Neurog2 during neuronal transcription. The Neurog2-regulated H3K9 demethylation via association with KDM3A ensures proper neuronal transcription. Our current findings also reveal that KDM3A is selectively required for Neurog2- but not for Ascl1-initiated neuronal transcription.

RESULTS

Expression of KDM3A is required for increasing the neurogenic potential of the naïve ectoderm in *Xenopus*

To delineate the function of KDM3A in early vertebrate development, we investigated the expression pattern of *kdm3a* mRNA in early *Xenopus* embryos. Whole-mount *in situ* hybridization indicated that *kdm3a* mRNA was expressed throughout early *Xenopus* development. During the cleavage to gastrula stages, *kdm3a* was detected in the animal hemisphere (Fig. 1A,B), from which the neural ectoderm emerges. During the early neurula stage, *kdm3a* was ubiquitously expressed with a slight enrichment in the CNS (Fig. 1C). At later stages of development, *kdm3a* was more obviously enriched in the CNS (Fig. 1D,E), particularly in the anterior parts of the CNS, including the eye fields. These data suggest that KDM3A is expressed in the right place at the right time to regulate neural development in *Xenopus*.

To study the function of KDM3A in neural development, we analyzed the effects of KDM3A depletion using a translation-blocking morpholino oligo (MO) that recognizes the start codon-spanning sequences of *kdm3a* mRNA (Fig. S1A). A 5 bp mismatch mutant of this MO (cMO) was used as a control for MO specificity (Fig. S1A). The efficacy of KDM3A MO (3A MO) was verified using western blot analysis with an antibody directed against KDM3A. Microinjection of 3A MO (80 ng) into both cells at the two-cell stage resulted in a marked decrease of KDM3A protein from the mid-gastrula (stage 11) to the neural tube closure stage (stage 18) (Fig. 1F), confirming that the KDM3A MO is an efficient tool for assessing the function of KDM3A during crucial stages of neural development in *Xenopus*. By contrast, microinjection of the same dose of cMO did not affect KDM3A expression (Fig. 1G). To determine whether KDM3A is involved in neural development, we took advantage of the animal cap assay. The naïve ectoderm dissected from the animal pole of mid-blastula stage embryos is pluripotent and can be directed into neural stem cells or neuronal fates, depending on signals provided. We compared the responsiveness of 80 ng cMO- or 3A MO-injected animal caps with the BMP antagonist noggin and other neural inducers. Using qPCR, we found that depletion of KDM3A did not discernably affect the ability of noggin to induce the expression of neural stem cell marker genes in the SoxB1 class (Fig. S1B), suggesting that KDM3A is dispensable for the BMP antagonist-mediated neural induction. However KDM3A depletion diminished the ability of FGF8a to activate neuronal genes, including *neurog2*, *neurod1*, *ebf2* and *tubb2b* (Fig. 1H). Interestingly, the ability of FGF8a to induce expression of the neural stem cell marker *sox2* and the pan-mesodermal gene *brachyury* (*t*) was not discernably affected (Fig. 1H). Additional analysis indicated that KDM3A was not required for the activin-induced mesoderm differentiation (Fig. S1C). These data collectively suggest that KDM3A is specifically required for the neurogenic potential of naïve ectoderm but not the neural induction per se. To elaborate on this, we analyzed the responsiveness of the naïve ectoderm to the overexpressed Neurog2 and Ascl1. First, we verified that ectopic expression of Myc-tagged Neurog2 or Ascl1 (MT-Neurog2, MT-Ascl1) was not affected by co-injection of either cMO or KDM3A MO (Fig. S1D,E). Intriguingly, using qPCR, we found that depletion of KDM3A differentially affected abilities of Neurog2 and Ascl1 to induce target gene expression. Ectopic Ascl1 exhibited comparable activities in cMO- or 3A MO-injected explants to stimulate the expression of several neuronal genes (Fig. 1I). By contrast, Neurog2 failed to activate neuronal genes, including *neurod1*, *neurod4*, *ebf2* and *tubb2b* when KDM3A was depleted (Fig. 1J), suggesting that KDM3A is specifically necessary for the neuronal transcription by Neurog2 but not for Ascl1-induced neuronal gene expression. Injecting the MO-resistant *kdm3a* mRNA restored the expression of KDM3A protein (Fig. 1G) and the ability of FGF8a and Neurog2 to induce target gene expression (Fig. 1H,J), suggesting that the KDM3A MO-mediated depletion effects are specific.

KDM3A depletion results in defective primary neurogenesis in early *Xenopus* embryos

Primary neurogenesis in *Xenopus* begins as soon as the neural plate has emerged, lasting up to the larva stages (Thuret et al., 2015). Early-born neurons from primary neurogenesis are essential for adoptive behaviors of the larva stage animals. Primary neurons can be conveniently identified by virtue of characteristic expression of neuronal marker genes, including *neurod1*, *myt1* and *tubb2b* (also known as neural tubulin), among others during neural fold to neural tube stages (Bellefroid et al., 1996; Ma et al., 1996; Moody et al., 1996; Talikka et al., 2002). To verify whether KDM3A plays a role in primary neurogenesis, we sequentially injected 40 ng cMO or 3A MO and mRNA encoding KDM3A (300 pg), together with 200 pg β-galactosidase (β-gal) mRNA into one cell at the two-cell stage (Fig. 2A). Embryos at stage 24/25 were then subjected to red-Gal staining followed by whole-mount in situ hybridization for *tubb2b* (Fig. 2B). We found that the expression of *tubb2b* in KDM3A morphants was markedly reduced (Fig. 2B,B′). Injecting the MO-resistant *kdm3a* mRNA partially rescued the *tubb2b* expression in KDM3A morphants (Fig. 2B,B′), indicating that

Development (2017) 144, 3674-3685 doi:10.1242/dev.144113

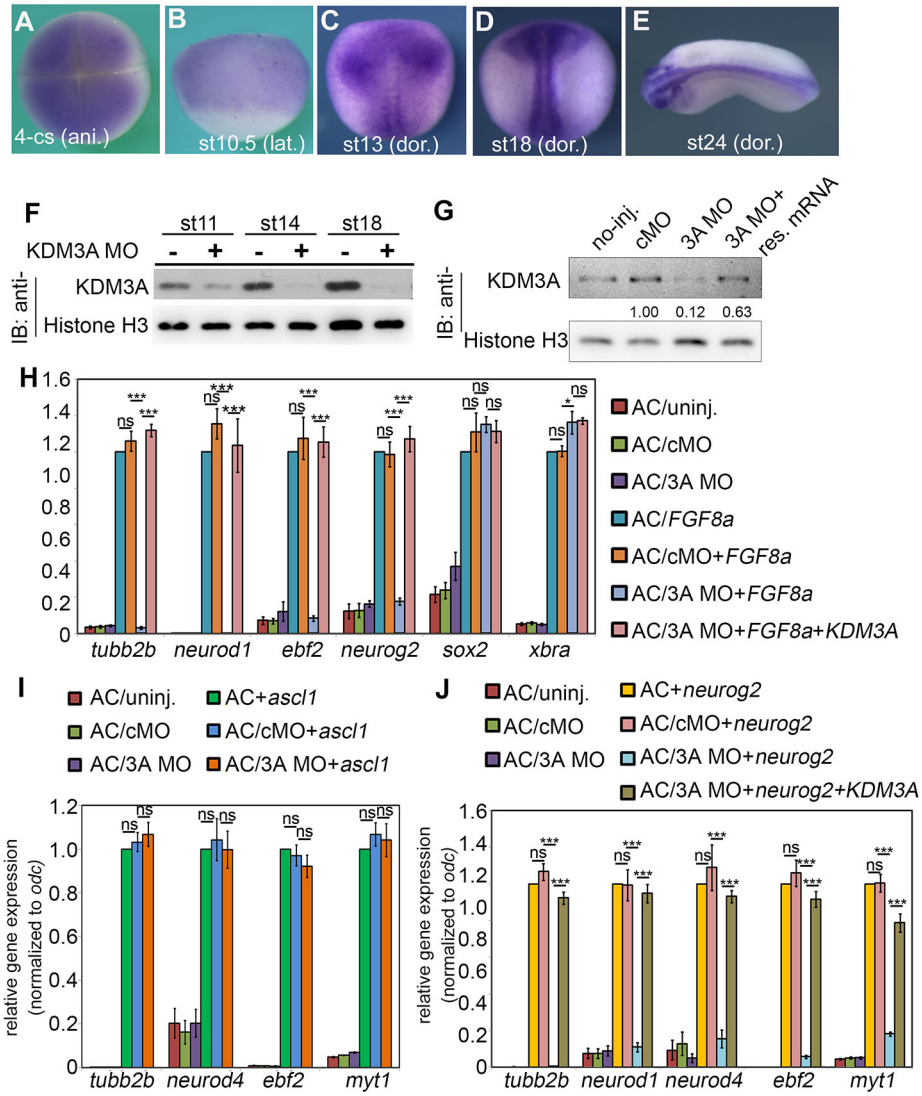

Fig. 1. Expression of KDM3A in early *Xenopus* embryos and the effects of its depletion on neurogenic potential. (A-E) The spatial expression pattern of *kdm3a* mRNA revealed through whole-mount *in situ* hybridization. (F) Western blot analysis of KDM3A in embryos injected with or without KDM3A MO (3A MO). 3A MO (80 ng) was injected into both cells at the two-cell stage. Embryos were then collected at the indicated stages (stage 11-18) and subjected to western blot analysis using an antibody directed against mouse KDM3A. Histone H3 served as a loading control. (G) Western blot analysis showing that injecting the MO-resistant *kdm3a* mRNA rescued the expression of KDM3A protein in 3A MO-injected embryos. Control MO (cMO) and 3AMO (60 ng) were injected into both cells at the two-cell stage. 3A MO-resistant *kdm3a* mRNA (500 pg) was injected at the one-cell stage. Embryos were then subjected to western blotting at stage 11. The numbers in G show the relative pixel intensities of bands when the intensity of cMO-injected lane was set to 1.00. (H-J) RT-qPCR analyses for gene expression in animal cap explants (AC) with indicated treatments. cMO or KDM3A MO (80 ng) was injected at the one-cell stage. mRNA (100 pg) encoding FGF8a (H), Ascl1 (I) or Neurog2 (J) was injected into animal pole of control embryos or MO-injected embryos at the two-cell stage. Two biological repeats and three technical repeats for each biological repeat were performed. The results from these six repeats were combined together and are represented as mean±s.e.m. The expression level of each examined gene in the group of animal cap explants (AC) that received only mRNA injection was set to 1 for normalization. Two-tailed Student *t*-test was performed to assess significance. ns, not significant. **P*<0.05; ****P*<0.005.

KDM3A is required for the primary neuron formation. Supporting this notion, KDM3A depletion also diminished the expression of other neuronal differentiation-related genes, including *neurod1*, *myt1* (a pan-neuronal marker), *HB9* (a marker of motor neurons), *islet1* (a marker of both motor and sensory neurons) and *xHox11L2* (a marker of Rohon-Beard neurons) when examined at the neural tube-closing stage (Fig. S2A). In line with the notion that KDM3A is dispensable for the transition of naïve ectoderm to neural stem/progenitor cells, we found that expression of the neural stem/progenitor markers such as *sox3* and *pax6* remained nearly normal in KDM3A morphants at the neural tube closing stage (Fig. S2B). Additional examination of marker genes at the late neurula stage (stage 18) indicated that KDM3A depletion did not discernibly affect the retina field formation or the anteroposterior pattern formation of neural tube (Fig. S2B). Moreover, the expression of representative markers for the neural plate border, neural crest specification and epidermis did not seem to be discernibly altered by KDM3A depletion (Fig. S2C). We noticed that expression patterns of *msx1*, *zic1* and *xk81b2* appeared somewhat differently in KDM3A morphants (Fig. S2C). This was likely due to the neural tube closure delay caused by KDM3A depletion (Fig. S2D), which could be partially rescued by re-injection of the MO-resistant *kdm3a* mRNA (Fig. S2D). These data together confirmed the notion that KDM3A is not required for neural induction per se but is necessary for neuronal differentiation *in vivo*. Importantly, reinjection of the 3A MO-resistant *kdm3a* mRNA could partially rescue the expression of *tubb2b* in KDM3A morphants (Fig. 2B,B′) and the neural tube closure (Fig. S2D), strongly suggesting that the observed neuronal defects are specifically due to KDM3A depletion.

To verify whether KDM3A is required for primary neuron induction by proneural factors in the bHLH family, we sequentially injected 40 ng 3A MO and *neurog2* or *ascl1* mRNA (50 pg for each) together with β-*gal* (200 pg) into a single cell at the two-cell stage and examined the expression of *tubb2b* during the neural fold stages (stage 16/17). We observed that KDM3A depletion abolished the ability of Neurog2 to induce ectopic expression of *tubb2b* (Fig. 2C,C′). By contrast, Ascl1 remained able to induce ectopic neuronal formation in the KDM3A-depleted embryos (Fig. 2C,C′). Furthermore, KDM3A depletion also drastically diminished the abilities of *Xenopus* neurogenin 1 (Xneurog1), neurogenin3 (Xneurog3) and mouse Neurog2 to induce ectopic neuron formation (Fig S3A and B), indicating that KDM3A is required for all these tested neurogenin factors to induce neuronal formation.

To additionally address the specificity of KDM3A depletion, we designed a second MO (KDM3A MO2) recognizing the *kdm3a* 5′ UTR region (Fig. S3C). Microinjection of KDM3A MO2 (40 and

Development (2017) 144, 3674-3685 doi:10.1242/dev.144113

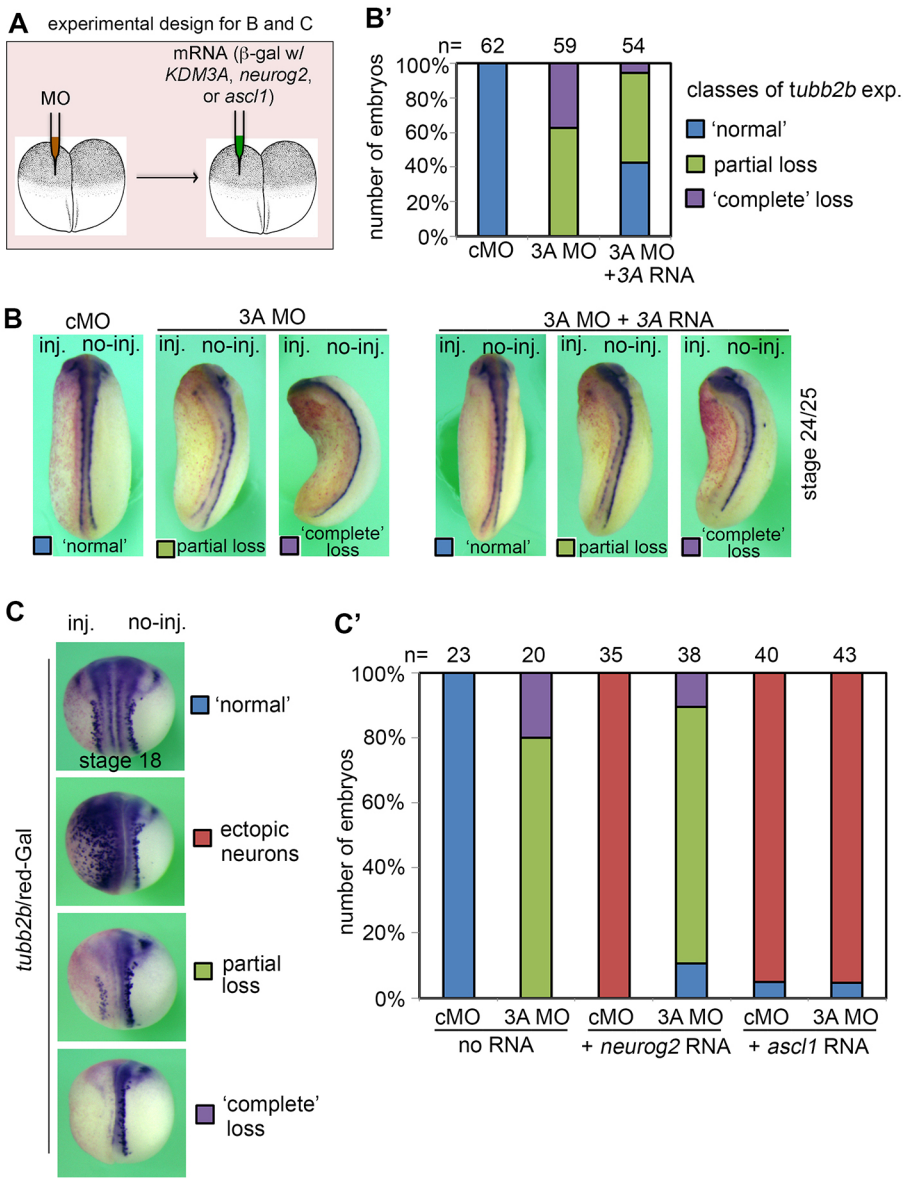

Fig. 2. KDM3A is required for the primary neurogenesis in *Xenopus*. (A) A schematic showing the experimental design for B and C. (B,B′) Embryos at stage 24/25 stained with red-Gal and *in situ* hybridized with *tubb2b*. cMO or 3A MO (40 ng) was injected into one cell at the two-cell stage. The 3A MO-resistant *kdm3a* mRNA (300 pg) together with 200 pg β-*gal* mRNA was subsequently injected into the 3A MO-injected cell at the two-cell stage. The expression levels of *tubb2b* were classified into three categories: 'normal', as seen in cMO-injected embryos; 'partial', as seen in some of KDM3A depleted embryos; and 'complete' loss, as seen in the remainder of the KDM3A-depleted embryos. Injection of the MO-resistant *kdm3a* mRNA partially rescues the expression of *tubb2b* in KDM3A morphants. The numbers on the top of histograms in B′ are sums from two independent experiments. (C,C′) Embryos at stage 16/17 stained with red-Gal and *in situ* hybridized with *tubb2b*. cMO and 3A MO (40 ng) were injected into one cell at the two-cell stage. mRNA (100 pg) encoding *neurog2* or *ascl1* together with 200 pg β-*gal* mRNA was subsequently injected into the MO-receiving cell at the two-cell stage. Phenotypes were classified into four categories based on whether ectopic neurons were induced and/or whether *tubb2b* was 'partially' or 'completely' lost in the MO-injected side. The numbers on the top of histograms in C′ are the total number of samples from two independent experiments.

80 ng) at the two-cell stage also markedly depleted the KDM3A expression in late gastrulae (Fig. S3D). Microinjection of the KDM3A MO2 reproduced the effects of 3A MO, including abolishing the ability of ectopic Neurog2 (50 pg mRNA) to induce expression of several neuronal genes in the naïve ectoderm explants (Fig. S3E), diminishing the expression of *tubb2b* (Fig. S3F), slowing down neural tube closure and causing a defect in the eye formation (Fig. S3F). Injecting MO-resistant *kdm3a* mRNA (300 pg) partially rescued the *tubb2b* expression, the neural tube closure delay and eye formation in the 3A MO2-injected embryos (Fig. S3F), reaffirming that KDM3A is specifically required for neurogenesis in *Xenopus*. Taken together, we conclude that KDM3A is essential for primary neurogenesis in *Xenopus*.

Neurog2 fails to transactivate neuronal genes in KDM3A-depleted embryos

It has been established that Neurog2 plays a hierarchical role in initiating the formation of neuronal precursors and subsequent differentiation (Ma et al., 1996). We therefore investigate the expression of Neurog2 and its targets in KDM3A morphants. Both whole-mount *in situ* hybridization and qPCR analyses revealed that Neurog2 was activated in nearly normal levels in KDM3A-depleted embryos at late neurula stages (Fig. 3A,B), suggesting that KDM3A depletion mainly affects the differentiation capacity of neuronal precursors. Consistent with this notion, we found that ectopic Neurog2 was able to induce ectopic expression of *neurod1* (Fig. 3C) and *myt1* (Fig. S4A) in 80 ng cMO-injected embryos, but failed to do so in 80 ng KDM3A MO-injected embryos (Fig. 3C, Fig. S4A). Moreover, KDM3A depletion also markedly blocked the ability of murine Neurog2 to induce the expression of *tubb2b* (Fig. S3A) and *neurod1* (Fig. S3B). Because Neurog2 has been shown to integrate multiple environmental signals during neuronal differentiation (Bellefroid et al., 1996; Ma et al., 1996), we also tested depletion effects of KDM3A on retinoic acid (RA) and FGF8. We found that the activities of RA and FGF8 to induce ectopic neuron formation were abolished in embryos depleted of KDM3A (Fig. S4B; data not shown). These data together indicate that KDM3A is required for primary neurogenesis through Neurog2-mediated neuronal differentiation programs.

Development (2017) 144, 3674-3685 doi:10.1242/dev.144113

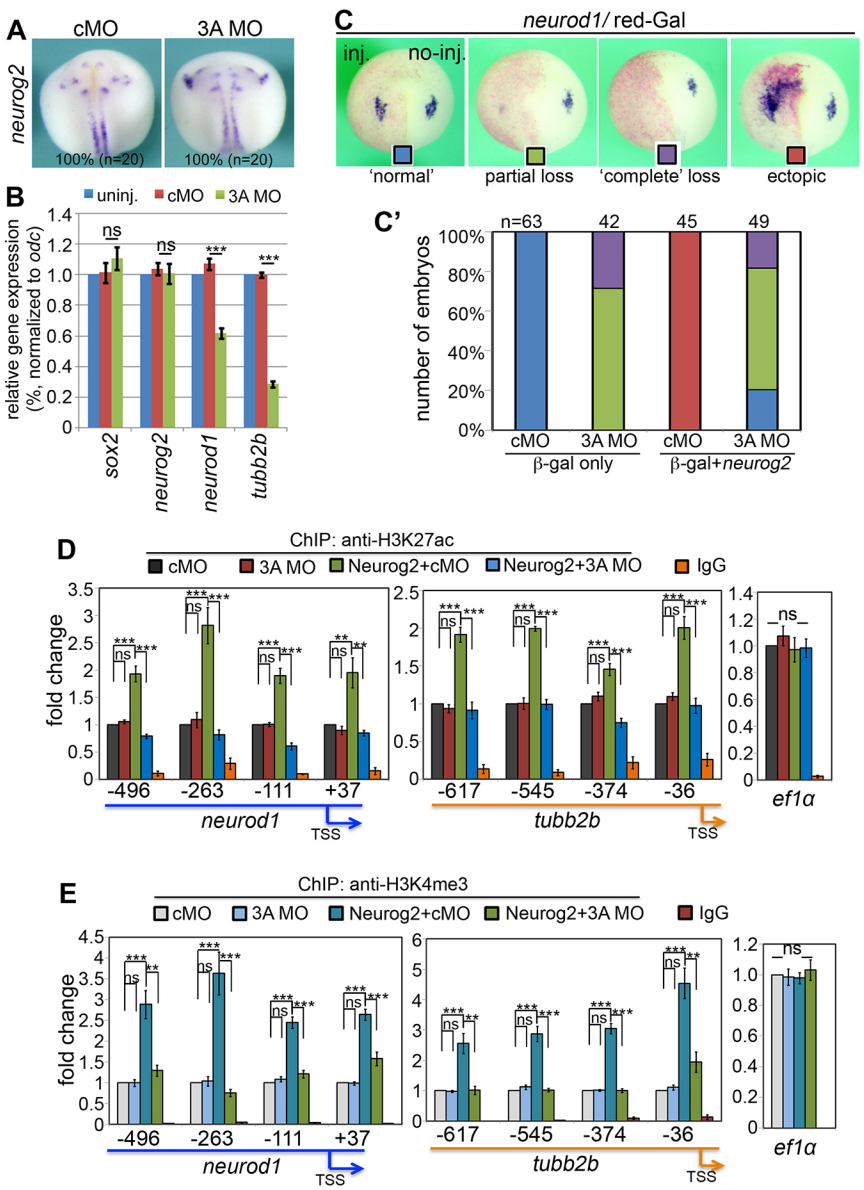

Fig. 3. Neurog2 fails to transactivate its neuronal targets in KDM3A morphant embryos. (A) Embryos at stage 17/18 *in situ* hybridized with *Xenopus neurog2*. cMO or 3A MO (80 ng) was injected into both cells at the two-cell stage. (B) qPCR results showing that KDM3A depletion differentially affects the expression of neural progenitor genes (*sox2* and *neurog2*) and neuronal genes (*neurod1* and *tubb2b*). ns, no significance. ***P<0.001. cMO or 3A MO (80 ng) was injected into both cells at the two-cell stage. Embryos were processed for RT-qPCR at stage 16. (C,C′) Embryos at stage 18 stained with red-Gal and *in situ* hybridized with *neurod1*. cMO or 3A MO (40 ng) was injected into one cell at the two-cell stage. mRNA encoding Neurog2 (100 pg) together with 200 pg β-*gal* mRNA was subsequently injected into the MO-receiving cell at the two-cell stage. (D,E) ChIP-qPCR detection of H3K27ac (D) and H3K4me3 (E) at the *neurod1* and *tubb2b* promoters. cMO or 3A MO (80 ng) was injected into one-cell stage embryos. mRNA encoding Neurog2 (100 pg) was injected into both cells of half of the MO-injected embryos at the two-cell stage. *ef1α* expression was examined as a negative control. Locations of the qPCR primers are schematically shown in the *x* axes. The ChIP-qPCR experiments shown in D,E were combined from two independent repeats. Three technical replicates were made in each independent repeat. **P<0.01; ***P<0.005; ns, not significant (according to a two-tailed Student's *t*-test).

It has been shown that, during neurogenesis in the mouse spinal cord, Neurog2 is able to recruit CBP and establish the acetylated H3 marks at neuronal genes (Lee et al., 2009). Neurog2 has also been shown to promote H3K4me3 marks at neuronal genes (Lee et al., 2009). In order to determine whether KDM3A depletion affects H3K27ac or H3K4me3 deposition at the Neurog2-responsive neuronal genes, we performed anti-H3K27ac and anti-H3K4me3 ChIP followed by qPCR analyses. To do this, we sequentially injected 80 ng cMO or KDM3A MO at the one-cell stage and then 100 pg *neurog2* mRNA into both cells at the two-cell stage. ChIP-qPCR analyses were performed when embryos developed to the late neurula stage (stage 18). We verified that ectopic Neurog2 significantly increased the deposition of H3K27ac (Fig. 3D) and H3K4me3 (Fig. 3E) at the *neurod1* and *tubb2b* promoters. KDM3A depletion alone did not discernably alter H3K27ac or H3K4me3 marks at the *neurod1* and *tubb2b* promoters (Fig. 3D,E). However, KDM3A depletion markedly reduced the ectopic Neurog2-promoted deposition of H3K27ac (Fig. 3D) and H3K4me3 (Fig. 3E) at the examined neuronal loci. These data together confirm that KDM3A is required for Neurog2 to transactivate its target genes.

KDM3A interacts with Neurog2

Our analyses thus far suggest that KDM3A might function together with Neurog2 to promote neuronal differentiation. To determine whether *Xenopus* Neurog2 interacts with KDM3A, we performed co-immunoprecipitation using embryonic lysates overexpressing epitope tagged-Neurog2 and KDM3A, or their deletion mutants (Fig. 4A). We found that 6MT-KDM3A could be detected in the immunocomplex precipitated by anti-HA-Neurog2 antibody (Fig. 4B), indicating that Neurog2 is able to associate with KDM3A. The C-terminal domain deletion mutant of Neurog2 (Neurog2-ΔC) failed to precipitate KDM3A; however, the N-terminal domain deletion mutant of Neurog2 (Neurog2-ΔN) remained able to bind KDM3A (Fig. 4C), revealing that the C-terminal domain of Neurog2 is necessary for the interaction. Furthermore, we found that deletion of the N-terminal domain of KDM3A (KDM3A-ΔN) abolished the interaction with Neurog2 (Fig. 4D), indicating that the N-terminal domain of KDM3A is involved in the interaction. For comparison, we also investigated whether Ascl1 is able to associate with KDM3A. Using the same experimental designs, we did not find evidence that Ascl1 interacts with KDM3A (data not shown).

Development (2017) 144, 3674-3685 doi:10.1242/dev.144113

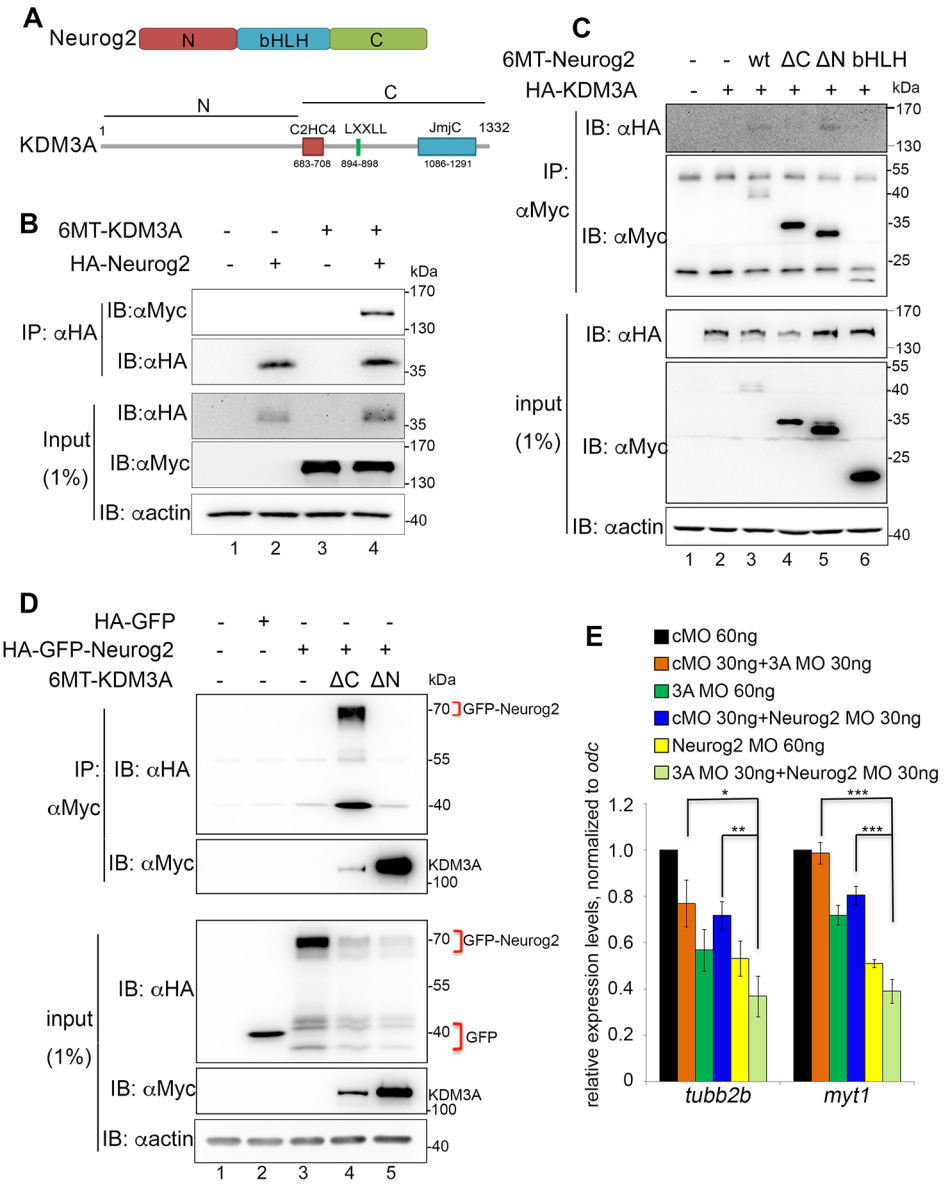

Fig. 4. KDM3A is associated with Neurog2. (A) Schematics of the domain organization of Neurog2 and KDM3A proteins. (B-D) CoIP followed by western blot analyses for the interaction between Neurog2 and KDM3A. mRNAs encoding the full-length epitope-tagged Neurog2 and KDM3A (B), deletion mutants of Neurog2 and the full-length KDM3A (C), or the full-length Neurog2 and deletion mutants of KDM3A (D) were microinjected into two-cell stage embryos, which were then collected at stage 14 and subjected to CoIP followed by western blot analyses with indicated antibodies. Bands around the 55 kDa and 40 kDa marks in the top blot are non-specific. (E) qPCR analysis of gene expression in cMO-, 3A MO- or Neurog2 MO-injected embryos. cMO, 3A MO or Neurog2 MOs with were injected into one-cell stage embryos at indicated doses followed by RT-qPCR for *tubb2b* and *myt1* expression at stage 16. **P*<0.05; ***P*<0.01; ****P*<0.005 (two-tailed Student's *t*-test). Doses of mRNAs injected for CoIP in B-D were 3 ng 6MT-KDM3A and 1.5 ng HA-Neurog2 (B); 3 ng HA-KDM3A, 0.5 ng WT Neurog2, 1.5 ng Neurog2-ΔC, 0.3 ng Neurog2-ΔN and 1.5 ng bHLH (C); and 50 pg HA-GFP, 1.5 ng HA-GFP-Neurog2, 3 ng 6MT-KDM3A-ΔC and 50 pg 6MT-KDM3A-ΔN (D). Numbers by the blots shown in B-D indicate the positions of molecular weight.

We then asked whether KDM3A interacts with mammalian Neurog2. To answer this, we used the neuronal cells derived from mouse NE-4C cells treated with retinoic acid (RA) and the neural stem cells derived from the H9 human stem cell line (see the supplementary Materials and Methods for detailed experimental procedures). We found that endogenous KDM3A and Neurog2 were detected in the same immunocomplex brought down by anti-KDM3A antibody (Fig. S4C), suggesting KDM3A interacts with mammalian Neurog2. These data collective indicate that KDM3A is a candidate co-factor for the proneural factors in the neurogenin subfamily.

The association between Neurog2 and KDM3A suggest that Neurog2 and KDM3A might cooperate to activate neuronal genes. To test this notion, we depleted Neurog2 using a previously characterized Neurog2 MO (Klisch et al., 2006) with or without additional depletion of KDM3A. Injection of Neurog2 MO alone at a lower dose (30 ng) only moderately reduced the expression of *myt1* and/or *tubb2b* (Fig. 4E). However, co-injection of 30 ng Neurog2 MO and 30 ng KDM3A MO together could significantly inhibit the expression of these neuronal genes (Fig. 4E), validating the notion that Neurog2 collaborates with KDM3A during neuronal gene activation. Together, we conclude that KDM3A physically and functionally interacts with Neurog2 during primary neurogenesis in *Xenopus*.

Neurog2 recruits KDM3A to demethylate H3K9me2 at the *neurod1* promoter

Recent progress has provided evidence that Neurog2 and Ascl1 initiate non-overlapping genetic programs during the conversion of non-neural cells into functional neurons (Masserdotti et al., 2015; Raposo et al., 2015; Wapinski et al., 2013). Our current findings suggest that KDM3A is selectively required for Neurog2 but not for Ascl1 to initiate neuronal programs. NeuroD1, a crucial regulator of neurogenesis, is a direct target of Neurog2 (Mattar et al., 2004; Miyata et al., 1999; Ozen et al., 2007; Sommer et al., 1996; Talikka et al., 2002). We exploited this fact further for better understanding how KDM3A is specifically involved in Neurog2-regulated neuronal differentiation. While overexpression of Neurog2 but not Ascl1 was able to induce *neurod1* expression in the naïve ectoderm (Fig. S5A,B), depletion of Ascl1, using a previously characterized

Development (2017) 144, 3674-3685 doi:10.1242/dev.144113

splice-blocking MO (Gao et al., 2016), markedly inhibited the expression of neuronal genes, including *tubb2b*, *myt1* and *neurod1* (Fig. S5C,C′). This is in accordance with our previous finding that Ascl1 is a competence factor for neurogenesis in *Xenopus* (Gao et al., 2016). Interestingly, our ChIP-qPCR analyses revealed that overexpressed Ascl1, like Neurog2 (Fig. 5A), could also bind the upstream regulatory region of *neurod1* (Fig. 5B). Ectopic Ascl1 only slightly enhanced the KMD3A binding around the −263 bp position relative to the transcription start site (TSS) of *neurod1* promoter (Fig. 5C). However, ectopic Ascl1 failed to reduce H3K9me2 levels from the *neurod1* promoter region that has been examined (Fig. 5D). By contrast, Neurog2 markedly enhanced the KDM3A binding at all examined locations (Fig. 5C) and concurrently reduced the deposition of H3K9me2 at these locations of the *neurod1* promoter (Fig. 5D), demonstrating that Neurog2 specifically facilitates recruitment of KDM3A to *neurod1*. Conversely, depletion of Neurog2 reduced the binding of KDM3A (Fig. 5E) and concomitantly increased the expression of H3K9me2 at *neurod1* (Fig. 5F). By contrast, depletion of Ascl1 did not discernably change levels of the H3K9me2 marks at the *neurod1* promoter (Fig. S5D). We noticed that Ascl1 depletion resulted in a noticeable but insignificant increase of H3K9me2 at the −36 position relative to the TSS of *tubb2b* promoter (Fig. S5E). Results from additional ChIP-qPCR experiments indicated that overexpressed Ascl1 did not enhance the recruitment of KDM3A to the −36 position of *tubb2b* promoter (Fig. S5F). It is thus possible that other H3K9 demethylase(s) are involved in the Ascl1-induced expression of *tubb2b*. These analyses indicate that KDM3A is a chromatin regulator specifically used by Neurog2 during the activation of *neurod1* expression. To further strengthen this notion, we examined overexpression effects of Neurog2 and Ascl1 on the promoter region of *myt1*, which is a common target of Neurog2 and Ascl1 (Seo et al., 2007; Vasconcelos et al., 2016). We verified through ChIP-qPCR that both ectopic Neurog2 and Ascl1 were able to bind the promoter sequence of *myt1* (Fig. S5G). However, only overexpressed Neurog2 was able to increase the binding of KDM3A on the promoter region of *myt1* (Fig. S5H) and concomitantly decrease the H3K9me2 marks on the promoter region of *myt1*, but

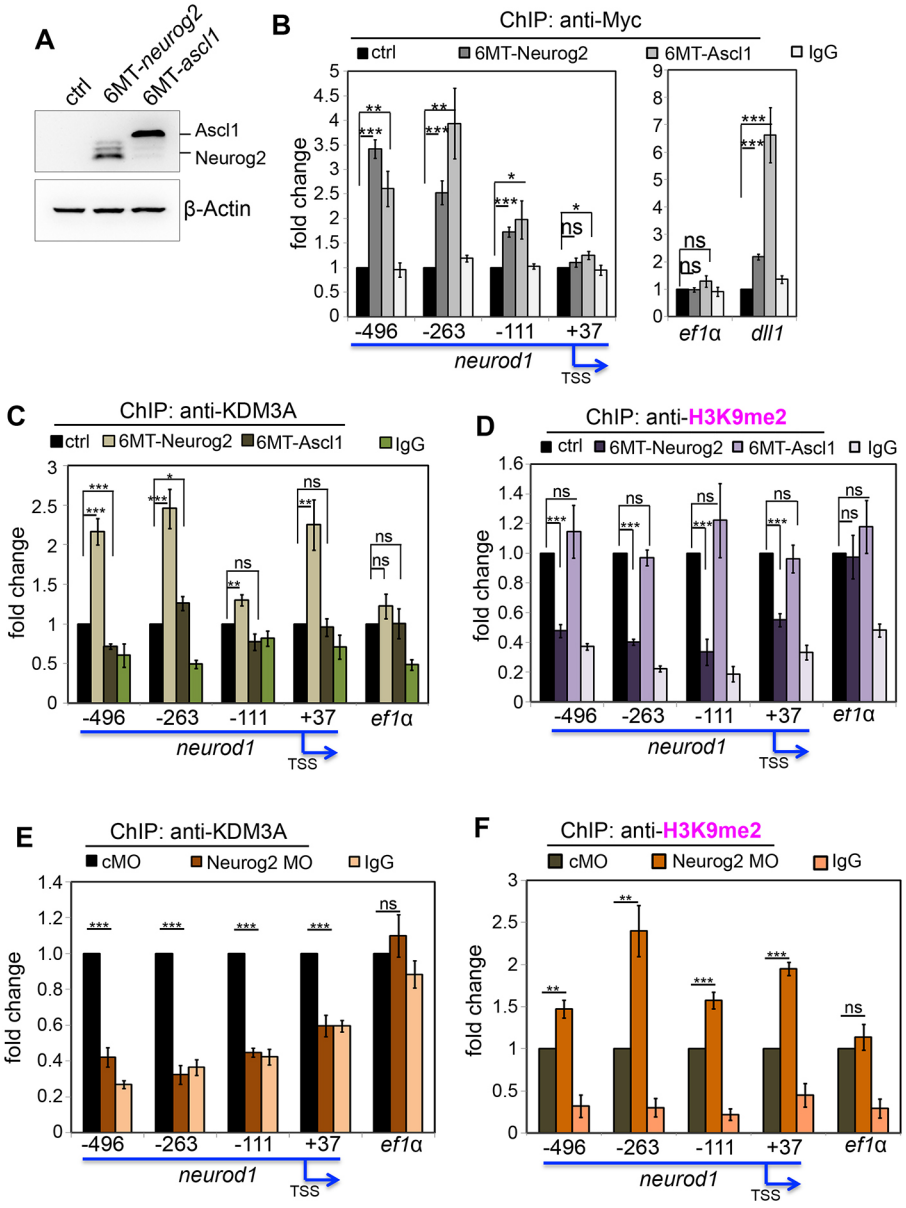

Fig. 5. Neurog2 recruits KDM3A to neuronal targets. (A) Western blot detection of MT-tagged proteins from embryos microinjected with mRNAs encoding 6MT-Neurog2 and 6MT-Ascl1. The doses of 6MT-*neurog2* (500 pg) and 6MT-*ascl1* (200 pg) mRNA were optimized to ensure both proteins ectopically expressed at comparable levels for the ChIP-qPCR experiments shown in B-D. (B) Anti-Myc ChIP followed by qPCR analyses at stage 15, indicating that overexpressed 6MT-Neurog2 and 6MT-Ascl1 were able to bind the promoter region of *neurod1* (left panel). *ef1*α and *dll1* (*delta-like* 1) served, respectively, as negative and positive controls. (C) Anti-KDM3A ChIP-qPCR analyses at stage 15, indicating that overexpressed Neurog2 but not Ascl1 could increase KDM3A bound on the promoter region of *neurod1*. (D) Anti-H3K9me2 ChIP-qPCR analyses at stage 18, indicating that overexpressed Neurog2 but not Ascl1 decreased the H3K9me2 marks on the *neurod1* promoter. (E) Anti-KDM3A ChIP-qPCR analyses at stage 15, indicating that Neurog2 MO (80 ng) but not standard MO reduced KDM3A bound on the *neurod1* promoter. (F) Anti-H3K9me2 ChIP-qPCR at stage 18 showing that Neurog2 MO (80 ng) but not standard MO increased the H3K9me2 marks on the *neurod1* promoter. The ChIP-qPCR experiments shown in B-F were combined from two biological repeats. Three technical replicates were made in each biological repeat. **P*<0.05; ***P*<0.01; ****P*<0.005; ns, not significant (two-tailed Student's *t*-test).

Development (2017) 144, 3674-3685 doi:10.1242/dev.144113

Ascl1 failed to do so (Fig. S5I). These data collectively reaffirmed the conclusion that KDM3A is specifically used by Neurog2 to decrease the H3K9me2 marks during neuronal activation.

We additionally verified that Neurog2 could also recruit KDM3A to the neuronal differentiation gene *tubb2b*. First, we confirmed that Neurog2 was able to directly transactivate *tubb2b* through dual-luciferase reporter assays (Fig S6A,B). ChIP-qPCR revealed that overexpressed Neurog2 bound the promoter region of *tubb2b* (Fig. S6C). Importantly, ectopic Neurog2 significantly decreased the deposition of H3K9me2 at the promoter region of *tubb2b* in cMO-injected embryos; however, it failed to do so in the KDM3A MO-injected embryos (Fig. S6D). Conversely, depletion of Neurog2 significantly reduced the binding of KDM3A (Fig. S6E) and increased the expression of H3K9me2 at the promoter region of *tubb2b* (Fig. S6F), affirming that Neurog2 is able to recruit KDM3A and demethylate H3K9me2 at its targets that are important for neuronal differentiation. Taken together, we conclude that Neurog2 is able to recruit KDM3A to its targets and promote H3K9me2 demethylation around its binding sites.

KDM3A regulates Neurog2 recruitment to its targets

Having established a role for Neurog2 in recruitment of KDM3A to its target neuronal genes, we then sought to investigate how KDM3A regulates the transactivity of Neurog2. Consistent with reports from others (Yamane et al., 2006; Loh et al., 2007), we found that overexpression of KDM3A by injecting a high dose of *kdm3a* mRNA (2 ng) in early *Xenopus* embryos decreased the expression level of soluble H3K9me2 and to some extent that of H3K9me1 (Fig. 6A). Interestingly, we observed through a series of ChIP-qPCR analyses that ectopic expression of KDM3A, but not of an enzymatically dead mutant (KDM3A H1130Y) (Yamane et al., 2006), reduced levels of the H3K9me2 marks at the *neurod1* and *tubb2b* promoters (Fig. S7A,B), suggesting that KDM3A overexpression is able to modulate H3K9me2 at these neuronal genes. However, simple overexpression of KDM3A was not sufficient for the establishment of H3K27ac at *neurod1* or *tubb2b* (Fig. S7C,D). Consistently, whole-mount *in situ* hybridization revealed that ectopic KDM3A did not discernably change the expression of *tubb2b* or *neurod1* (Fig. 6B), suggesting KDM3A

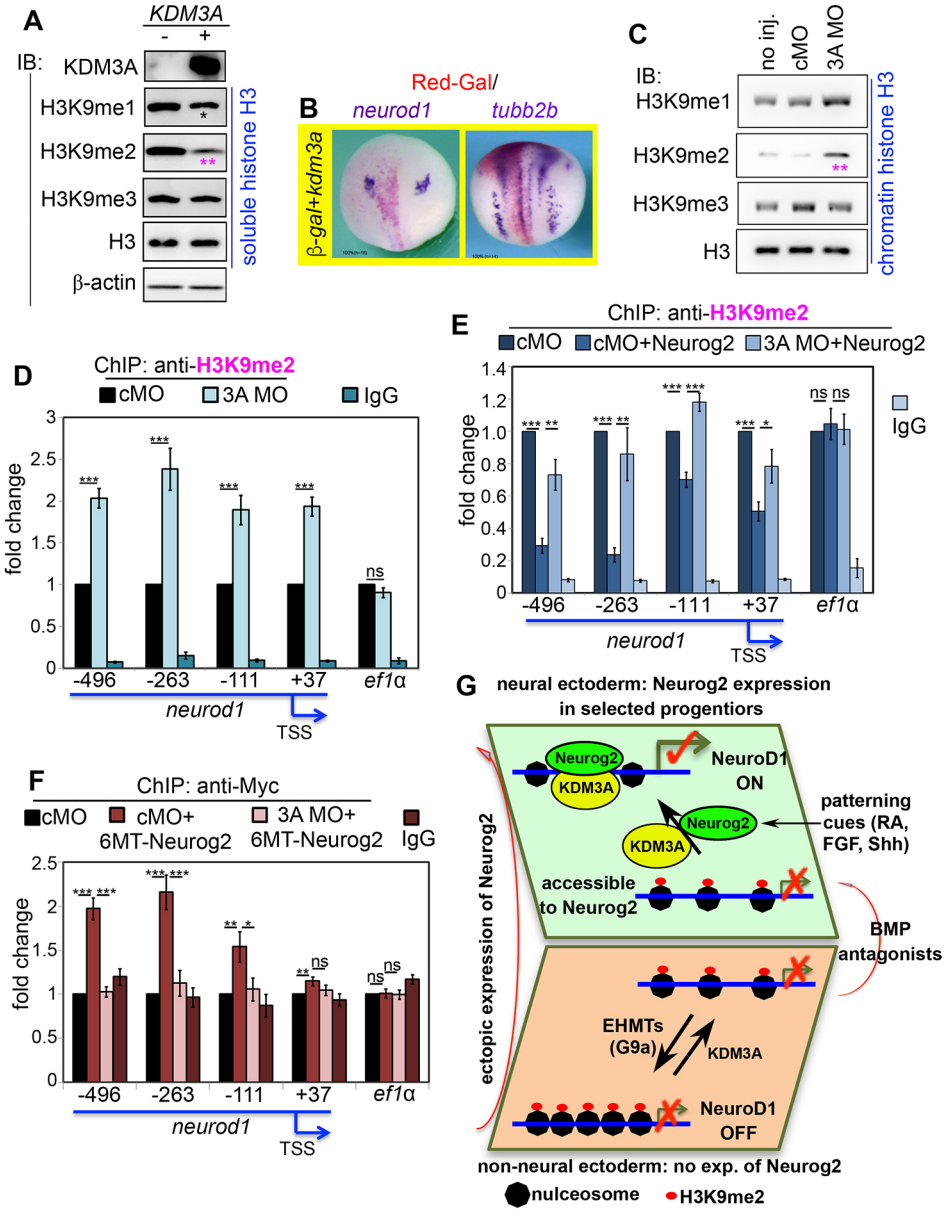

Fig. 6. KDM3A-mediated demethylation of H3K9me2 enhances Neurog2 recruitment at the *neurod1* promoter. (A) Western blot detection of soluble histone H3, H3K9me1, H3K9me2 and H3K9me3 in control and 2 ng *kdm3a* mRNA-injected embryos. (B) Embryos stained with red-Gal and *in situ* hybridized with *neurod1* (left panel, stage 18) or *tubb2b* (right panel, stage 15). β-*gal* (200 pg) together with 1 ng *kdm3a* was injected into one cell at the two-cell stage. (C) Western blot detection of chromatin histone H3, H3K9me1, H3K9me2 and H3K9me3 in embryos without injection or injected with 80 ng cMO or 3A MO. See Materials and Methods for isolation of chromatin histones. (D) Anti-H3K9me2 ChIP-qPCR analyses showing that 80 ng KDM3A MO increased the H3K9me2 marks on the *neurod1* promoter. (E) Anti-H3K9me2 ChIP-qPCR analyses showing that Neurog2 was unable to reduce the H3K9me2 marks on the *neurod1* promoter when KDM3A was depleted by injecting 80 ng 3A MO. (F) Anti-Myc ChIP-qPCR analyses showing that ectopic Neurog2 was unable to bind the *neurod1* promoter when KDM3A was depleted (cMO or 3A MO: 80 ng). ChIP-qPCR results shown in D-F were combined from two biological repeats. Three technical replicates were made in each biological repeat. **P*<0.05; ***P*<0.01; ****P*<0.005, ns, not significant (two-tailed Student's *t*-test). (G) A summary of our current findings that posit the roles for KDM3A in regulating chromatin states and its collaboration with Neurog2 to initiate neuronal precursor differentiation. See details in the Discussion.

Development (2017) 144, 3674-3685 doi:10.1242/dev.144113

alone is not sufficient to activate neuronal genes. These observations are instead consistent with the notion that Neurog2 is rate limiting in the activation of these neuronal genes. Depletion of KDM3A resulted in a detectable increase of chromatin H3K9me2, as revealed by western blot analysis using a high-salt buffer with chloric acid extracted-chromatin protein from cMO- and 3A MO-injected embryos at the late neurula stage (Fig. 6C) (Tien et al., 2015). This was further supported by our ChIP-qPCR analyses of the promoter regions of *neurod1* (Fig. 6D) and *tubb2b* (Fig. S7E). Moreover, KDM3A depletion drastically reduced the ability of ectopic Neurog2 to decrease the expression of H3K9me2 at the promoters of *neurod1* (Fig. 6E) and *tubb2b* (Fig. S6D). To further determine how KDM3A regulates the activity of Neurog2, we investigated using ChIP-qPCR the binding of Neurog2 at its targets upon KDM3A depletion. We found that KDM3A depletion diminished the binding of Neurog2 at promoters of *neurod1* (Fig. 6F) and *tubb2b* (Fig. S7F). Taken together, we conclude that KDM3A-mediated demethylation of H3K9me2 is necessary for effective binding of Neurog2 at its target sites.

DISCUSSION

KDM3A, a well-characterized H3K9me2/1 demethylase, has been implicated in spermatogenesis and metabolism (Cheng et al., 2014; Herzog et al., 2012; Kuroki et al., 2013; Liu et al., 2010; Okada et al., 2007; Tateishi et al., 2009). In this study, we provided evidence that KDM3A is a novel co-factor for Neurog2 during neuronal precursor formation and differentiation in *Xenopus*. KDM3A interacts with Neurog2; the interaction involves the N-terminal sequence of KDM3A and the C-terminal domain of Neurog2. Depletion of KDM3A diminishes the abilities of Neurog2 to reduce the repressive H3K9me2 and to increase active histone marks in promoter regions of neuronal genes. Our study reveals that KDM3A is essential for primary neurogenesis in *Xenopus*. Our findings advance the understanding of the molecular mechanisms underlying proneural factor-initiated cell fate commitment and differentiation.

Neurog2, but not Ascl1, functionally interacts with KDM3A during neuronal transcription

Primary neurogenesis in *Xenopus* provides an excellent *in vivo* system for delineating the molecular mechanisms underlying neural fate specification and determination (Ma et al., 1996; Thuret et al., 2015). Expression of the proneural genes in the neurogenin subfamily during CNS development is regulated by environmental signals, including Shh, RA, FGF and the Notch/Delta lateral inhibition system (Chitnis, 1999; Koyano-Nakagawa et al., 1999; Moody et al., 1996). Neurog2 appears to be activated on time and its mediolateral expression pattern remains nearly normal in KDM3A morphants (Fig. 3A), suggesting that KDM3A is not required for the initial selection of neuronal precursors. Instead, KDM3A depletion diminishes the abilities of Neurog2, FGF8 and RA to induce neuronal gene expression (Fig. 1H,J, Fig. S4B), suggesting that the KDM3A-mediated histone H3K9me2/1 demethylation is essential for neuronal differentiation downstream of Neurog2 and other environmental cues. By analyzing the activation of several representative neuronal genes, our primary goal was to understand how Neurog2 and KDM3A jointly initiate neuronal precursor differentiation. To achieve this, Ascl1, a proneural factor in the *achaete-scute* subfamily, was compared in several respects. Interestingly, we found that Ascl1 remains capable of inducing expression of *neurod4* and *tubb2b* when KDM3A is depleted (Figs 1I and 2C), suggesting that KDM3A is selectively required for Neurog2-initiated neuronal differentiation. Supporting this notion, we provided evidence that Neurog2 interacts with KDM3A. Under the same experimental conditions, an association between Ascl1 and KDM3A was not detected (data not shown). Furthermore, we demonstrated that Neurog2 is required for KDM3A recruitment at neuronal gene loci. Neurog2 promotes H3K9me2 demethylation depending on the presence of KDM3A. Conversely, ectopic Ascl1 fails to modulate H3K9me2 marks at the promoters of *neurod1* or *myt1*, despite its detectable binding to these neuronal promoters. It has been demonstrated that Neurog2 and Ascl1 trigger *in vitro* neuronal transdifferentiation through non-overlapping genetic programs (Masserdotti et al., 2015; Raposo et al., 2015; Wapinski et al., 2013). Our current findings provide at least one additional angle to account the different transactivities of Neurog2 and Ascl1, i.e. Neurog2 but not Ascl1 is able to overcome the repressive effects of H3K9me2 on neuronal genes due to a specific interaction between Neurog2 and KDM3A. More-detailed structure-function analyses in the future will help to better understand how Neurog2 selectively uses KDM3A and modulates chromatin environment on site. We have previously shown that the pre-neurula stage expression of Ascl1 is also required for neurogenic potential and FGF8a-induced neuronal differentiation (Gao et al., 2016). Our current analyses indicate that Ascl1 transactivates its target genes likely in a KDM3A-independent manner. Because functional neurons induced by Neurog2 and/or Ascl1 hold great promise for regenerative medicine (Chen et al., 2015), further investigations on comparing the difference between Neurog2 and Ascl1 using the *Xenopus* model will continue to provide developmental principle-inspired improvements in neuronal transdifferentiation protocols (Ang and Wernig, 2014; Pang et al., 2011; Yang et al., 2011). Interestingly, our preliminary investigation indicates that KDM3A is upregulated during induced neuronal differentiation of human induced pluripotent stem cells.

KDM3A enhances chromatin-mediated recruitment of Neurog2 at neuronal gene loci

We found that KDM3A depletion increases H3K9me2 marks and reduces the binding of Neurog2 to its targets, suggesting that Neurog2 might not be able to stably bind closed chromatin. This points to an additional difference between Neurog2 and Ascl1, because Ascl1 has been shown to function as a pioneer transcription factor that is able to access closed chromatin (Vierbuchen et al., 2010; Wapinski et al., 2013). How does Neurog2 access and transactivate its target neuronal genes? We found that both H3K9me2 in the soluble pool and H3K9me2 associated with the neuronal gene loci are inversely correlated with KDM3A expression levels, implying that KDM3A may function through both Neurog2-independent and Neurog2-dependent fashion (Fig. 6G). The activity of KDM3A in both of these respects might be balanced by the H3K9-specific methylases such as G9a/GLP (Fuks et al., 2003; Smallwood et al., 2007; Snowden et al., 2002), allowing a suboptimal recruitment of Neurog2 at its targets. Recently, it has been proposed that histone turnover at chromatin is essential for neuronal transcription (Lee et al., 2009; Maze et al., 2013, 2015; Seo et al., 2005). Therefore, the enriched expression of KDM3A in the developing CNS may be involved in maintaining neuronal gene loci in primed states (Fig. 6G, lower panel), which facilitates the access to chromatin by Neurog2. The association of Neurog2 with KDM3A at regulatory regions of neuronal genes enhances the Neurog2 residence at its targets (Fig. 6G, upper panel), engendering the determinate activation of neuronal genes. This hypothesis is consistent with our data demonstrating that KDM3A overexpression alone is not sufficient to activate neuronal genes, and the notion that

Development (2017) 144, 3674-3685 doi:10.1242/dev.144113

Neurog2 is rate limiting for neuronal gene activation. The full activation of neuronal genes by Neurog2 likely also needs the recruitment of other types of histone-modifying enzymes, such as CBP and/or chromatin remodeling complexes (Lee et al., 2009; Maze et al., 2013; Seo et al., 2005). While KDM3A depletion alone does not affect the basal levels of H3K4me3 or H3K27ac at neuronal genes, we found that depletion of KDM3A compromises the ability of Neurog2 to establish H3K27ac and H3K4me3 at neuronal gene loci (Fig. 3D,E). Further studies are needed to determine in greater detail how Neurog2 coordinates removal of repressive histone marks on one hand and decoration of active histone marks on the other. Our current findings open a novel venue for deeper understanding the molecular mechanisms underlying the neuronal precursor determination triggered by proneural factors in the bHLH family.

Roles for KDM3A and H3K9me2 in neural development

H3K9 methylation (H3K9me2/3) is not only involved in safeguarding stable terminal differentiation, but also in regulating developmental gene expression in the right place at right time (Black et al., 2012; Soshnev et al., 2016). Our current analyses posit a specific role for KDM3A in neuronal differentiation. However, this does not exclude the possibility that H3K9me2 may function in broader developmental contexts. KDM3A is a maternal gene, the function of which remains unclear. Interestingly, it has been recently reported from others that chromatic H3K9me2/3 is not discernably detected until mid-gastrula stages (Wang et al., 2014b). Injection of KDM3A MO at the two-cell stage could reduce KDM3A protein with a concomitant increase of H3K9me2 from the mid-gastrula stage onwards (Fig. 1F; data not shown), implying that KDM3A is required for maintaining a proper level of expression of H3K9me2 during the early phases of embryonic cell fate allocation in *Xenopus*. However, the expression of neural stem cell markers did not seem to be affected in KDM3A morphants or in the naïve ectoderm explants treated with Noggin. Besides, the anteroposterior pattern formation of the CNS was retained in KDM3A morphants. Hence, we conclude that KDM3A and H3K9me2 are dispensable for the transition of naïve ectoderm to neural ectoderm. Instead, H3K9me2 might play a part in establishing chromatin states that subject neuronal genes to precise regulation by spatiotemporally controlled developmental cue (Black et al., 2012; Maze et al., 2013). It will be necessary to determine in future the genome-wide occupancy of KDM3A and/or H3K9me2 for better understanding the roles for KDM3A and H3K9me2 in regulating neural development. Moreover, different H3K9 demethylases in the JmjD1 (KDM3) subfamily may play different roles in neural development. Supporting this notion, KDM3C has been reported to repress neural differentiation of human embryonic stem cells (Wang et al., 2014a), suggesting that different KDM3 members might be used by different transcription factors during neural fate specification and differentiation. Our current findings strongly suggest that the joint actions of Neurog2 and KDM3A are essential for lowering the barrier of H3K9me2 against gene activation in the neuronal precursors (Fig. 6G).

Last but not least, KDM4A (also known as JmjD2A), a demethylase for H3K9me3, has been implicated in the neural crest specification in chick and frogs (Matsukawa et al., 2015; Strobl-Mazzulla et al., 2010). We found that KDM3A depletion does not discernably affect the expression of representative neural plate border genes and neural crest specification factors, indicating that KDM3A and perhaps H3K9me2 demethylation are dispensable for neural crest specification. Little attention has been paid to the difference between H3K9me2 and H3K9me3 in cell fate specification in literature (Black et al., 2012; Jamieson et al., 2016). Our current findings and the findings for KDM4A from others imply that the valence of H3K9 methylation may be differentially implicated in cell fate specification and determination.

MATERIALS AND METHODS

Frogs, embryos, animal cap assay and RT-qPCR analyses

The *Xenopus laevis* frogs were purchased from NASCO (Wisconsin) and reared in a temperature-controlled facility. Embryos were obtained through artificial insemination following standard procedures (Sive et al., 2000). For microinjection, fertilized eggs were dejellied at the one-cell stage using 2% cysteine (pH 8.0) followed by thorough washing in 0.1×MMR (Marc's Modified Ranger) and then transferred into 4% Ficoll/0.3×MMR. The injection scheme of MOs and mRNAs is indicated in figures and/or figure legends where appropriated. Animal caps were dissected embryos with desired treatments at the stage 8.5 and cultured to desired stages, as specified in the relevant figure legends. For RT-PCR analyses, 10 animal caps and/or two whole embryos for each treatment group were prepared and lysed with Tris-HCl/SDS/Proteinase K (pH 7.4) buffer supplemented with RNase inhibitors. The total RNA was then extracted using acidic phenol: chloroform, precipitated using 70% isopropanol and resuspended with 20 µl nuclease-free water. cDNA was made with 1 µl of RNA for each sample using SuperScript III reverse transcriptase Kit (Invitrogen #18080093). qPCR analyses were performed using the LightCycler 2.0 (Roche) following the manufacturer's instructions. All qPCR primers were optimized to obtain melting curves that can separate reverse transcriptase (RT)-containing samples from RT-minus and H_2O control samples following procedures provided by the manufacturer's instructions for the LightCycler (Roche) and described previously (Sive et al., 2000; Xanthos et al., 2002). All RT-qPCR data presented in Figs 1H-J, 3B and 4E were obtained through combining two independent biological repeats (i.e. repeated with embryos from two different females) with three technical replicates for each repeat and shown as mean±s.e.m. (standard error of mean). The two-tailed Student's *t*-test was performed to assess significance.

Whole-mount *in situ* hybridization and the dual-luciferase reporter assay

Embryos at desired stages were fixed with MEMFA followed by the standard procedures of whole-mount *in situ* hybridization (Sive et al., 2000). In cases where β-gal was co-injected for lineage tracing, as shown in Figs 2, 3C and 6B, the red-Gal staining was carried out before the whole-mount *in situ* hybridization procedures. All *in situ* hybridized embryos were then bleached with H_2O_2 for 12 h under fluorescent lights. Information of all cDNA constructs used for *in situ* probe labeling can be found in Table S1. The dual-luciferase reporter assay was performed following procedures provided in the supplementary Materials and Methods.

Co-immunoprepicitations and western blots

Embryos overexpressing *Xenopus* Neurog2 and/or KDM3A were lysed in RIPA buffer followed by co-immunoprepicitation (CoIP) procedures as described previously (Ding et al., 2013; Zhang et al., 2014). The immunocomplex was then differentiated in denaturing PAGE followed by western blotting analyses as described previously (Ding et al., 2013; Zhang et al., 2014). Chromatic histone H3 detection shown in Fig. 6C was performed by extracting the nuclear fraction of histone from cMO or KDM3A MO-injected embryos using trichloric acid. Titration of antibodies was as follows: 0.5 µg desired antibodies were used all CoIP experiments; anti-histone antibodies were used at 1:500 dilution; anti-Myc and anti-HA were used at 1:1000 dilution. All Co-IP and western blot experiments were repeated at least twice using embryos from different females. Information about all antibodies used in this study can be found in Table S2. Details of the experimental procedures for the CoIP of endogenous Neurog2 and KDM3A as shown in Fig. S4C can be found in the supplementary Materials and Methods.

Development (2017) 144, 3674-3685 doi:10.1242/dev.144113

ChIP-qPCR

ChIP-qPCRs were carried out following protocols described previously (Blythe et al., 2009; Gao et al., 2016). Detailed procedures can be found in the supplementary Materials and Methods. Fifty embryos were used for each sample for the ChIP procedures. All ChIP-qPCR experiments were repeated twice using different batches of embryos. Three technical replicates were made in each independent repeat. Results from six repeats were then combined and assessed for significance by performing the two-tailed Student's *t*-test. The results were then presented as mean±s.e.m. Information about all antibodies used for ChIP can be found in Table S2. For ChIP experiments, 1 µg of anti-Myc, anti-KDM3A, anti-H3K9me2, anti-H3K4me3 and anti-H3K27ac was used.

Oligos and primers

Sequence information for morpholino antisense oligos, PCR primers, ChIP-qPCR primers can be found in Table S3. All PCR-related raw data can be found in the Table S4.

Acknowledgements

We thank Dr B. Y. Mao (Kunming Institute of Zoology, Chinese Academy of Sciences, Kunming, China) for providing cDNA constructs.

Competing interests

The authors declare no competing or financial interests.

Author contributions

Conceptualization: G.L., Q.T.; Methodology: H.L., X.Z., L.G., A.A.K., G.L., Q.T.; Validation: Q.T.; Formal analysis: Q.T.; Investigation: H.L., G.C., L.S., Y.C., G.L., Q.T.; Resources: L.S., A.A.K., Y.C.; Writing - original draft: Q.T.; Writing - review & editing: Q.T.; Supervision: Q.T.; Project administration: Q.T.; Funding acquisition: Q.T.

Funding

This work was supported in part by grants from the National Natural Science Foundation of China (31371458 and 31571531 to Q.T.) and also partially funded by the MOE Key Laboratory of Protein Sciences at the Tsinghua University School of Life Sciences.

Supplementary information

Supplementary information available online at
http://dev.biologists.org/lookup/doi/10.1242/dev.144113.supplemental

References

Ang, C. E. and Wernig, M. (2014). Induced neuronal reprogramming. *J. Comp. Neurol.* **522**, 2877-2886.

Aravantinou-Fatorou, K., Ortega, F., Chroni-Tzartou, D., Antoniou, N., Poulopoulou, C., Politis, P. K., Berninger, B., Matsas, R. and Thomaidou, D. (2015). CEND1 and NEUROGENIN2 reprogram mouse astrocytes and embryonic fibroblasts to induced neural precursors and differentiated neurons. *Stem Cell Rep.* **5**, 405-418.

Bellefroid, E. J., Bourguignon, C., Hollemann, T., Ma, Q., Anderson, D. J., Kintner, C. and Pieler, T. (1996). X-MyT1, a Xenopus C2HC-type zinc finger protein with a regulatory function in neuronal differentiation. *Cell* **87**, 1191-1202.

Bertrand, N., Castro, D. S. and Guillemot, F. (2002). Proneural genes and the specification of neural cell types. *Nat. Rev. Neurosci.* **3**, 517-530.

Black, J. C., Van Rechem, C. and Whetstine, J. R. (2012). Histone lysine methylation dynamics: establishment, regulation, and biological impact. *Mol. Cell* **48**, 491-507.

Blanchard, J. W., Eade, K. T., Szűcs, A., Lo Sardo, V., Tsunemoto, R. K., Williams, D., Sanna, P. P. and Baldwin, K. K. (2015). Selective conversion of fibroblasts into peripheral sensory neurons. *Nat. Neurosci.* **18**, 25-35.

Blythe, S. A., Reid, C. D., Kessler, D. S. and Klein, P. S. (2009). Chromatin immunoprecipitation in early Xenopus laevis embryos. *Dev. Dyn.* **238**, 1422-1432.

Castro, D. S. and Guillemot, F. (2011). Old and new functions of proneural factors revealed by the genome-wide characterization of their transcriptional targets. *Cell Cycle* **10**, 4026-4031.

Chen, G., Wernig, M., Berninger, B., Nakafuku, M., Parmar, M. and Zhang, C. L. (2015). In vivo reprogramming for brain and spinal cord repair. *eNeuro* **2**, ENEURO.0106-15.2015

Cheng, M.-B., Zhang, Y., Cao, C.-Y., Zhang, W.-L., Zhang, Y. and Shen, Y.-F. (2014). Specific phosphorylation of histone demethylase KDM3A determines target gene expression in response to heat shock. *PLoS Biol.* **12**, e1002026.

Chitnis, A. B. (1999). Control of neurogenesis–lessons from frogs, fish and flies. *Curr. Opin. Neurobiol.* **9**, 18-25.

Ding, Y., Zhang, Y., Xu, C., Tao, Q.-H. and Chen, Y.-G. (2013). HECT domain-containing E3 ubiquitin ligase NEDD4L negatively regulates Wnt signaling by targeting dishevelled for proteasomal degradation. *J. Biol. Chem.* **288**, 8289-8298.

Fuks, F., Hurd, P. J., Deplus, R. and Kouzarides, T. (2003). The DNA methyltransferases associate with HP1 and the SUV39H1 histone methyltransferase. *Nucleic Acids Res.* **31**, 2305-2312.

Gao, L., Zhu, X., Chen, G., Ma, X., Zhang, Y., Khand, A. A., Shi, H., Gu, F., Lin, H., Chen, Y. et al. (2016). A novel role for Ascl1 in the regulation of mesendoderm formation via HDAC-dependent antagonism of VegT. *Development* **143**, 492-503.

Grande, A., Sumiyoshi, K., López-Juárez, A., Howard, J., Sakthivel, B., Aronow, B., Campbell, K. and Nakafuku, M. (2013). Environmental impact on direct neuronal reprogramming in vivo in the adult brain. *Nat. Commun.* **4**, 2373.

Greer, E. L. and Shi, Y. (2012). Histone methylation: a dynamic mark in health, disease and inheritance. *Nat. Rev. Genet.* **13**, 343-357.

Hemmati-Brivanlou, A., Kelly, O. G. and Melton, D. A. (1994). Follistatin, an antagonist of activin, is expressed in the Spemann organizer and displays direct neuralizing activity. *Cell* **77**, 283-295.

Heng, J. I.-T., Nguyen, L., Castro, D. S., Zimmer, C., Wildner, H., Armant, O., Skowronska-Krawczyk, D., Bedogni, F., Matter, J.-M., Hevner, R. et al. (2008). Neurogenin 2 controls cortical neuron migration through regulation of Rnd2. *Nature* **455**, 114-118.

Herzog, M., Josseaux, E., Dedeurwaerder, S., Calonne, E., Volkmar, M. and Fuks, F. (2012). The histone demethylase Kdm3a is essential to progression through differentiation. *Nucleic Acids Res.* **40**, 7219-7232.

Huang, C., Chen, J., Zhang, T., Zhu, Q., Xiang, Y., Chen, C. D. and Jing, N. (2010a). The dual histone demethylase KDM7A promotes neural induction in early chick embryos. *Dev. Dyn.* **239**, 3350-3357.

Huang, C., Xiang, Y., Wang, Y., Li, X., Xu, L., Zhu, Z., Zhang, T., Zhu, Q., Zhang, K., Jing, N. et al. (2010b). Dual-specificity histone demethylase KIAA1718 (KDM7A) regulates neural differentiation through FGF4. *Cell Res.* **20**, 154-165.

Jamieson, K., Wiles, E. T., McNaught, K. J., Sidoli, S., Leggett, N., Shao, Y., Garcia, B. A. and Selker, E. U. (2016). Loss of HP1 causes depletion of H3K27me3 from facultative heterochromatin and gain of H3K27me2 at constitutive heterochromatin. *Genome Res.* **26**, 97-107.

Klisch, T. J., Souopgui, J., Juergens, K., Rust, B., Pieler, T. and Henningfeld, K. A. (2006). Mxi1 is essential for neurogenesis in Xenopus and acts by bridging the pan-neural and proneural genes. *Dev. Biol.* **292**, 470-485.

Koyano-Nakagawa, N., Wettstein, D. and Kintner, C. (1999). Activation of Xenopus genes required for lateral inhibition and neuronal differentiation during primary neurogenesis. *Mol. Cell. Neurosci.* **14**, 327-339.

Kuroki, S., Matoba, S., Akiyoshi, M., Matsumura, Y., Miyachi, H., Mise, N., Abe, K., Ogura, A., Wilhelm, D., Koopman, P. et al. (2013). Epigenetic regulation of mouse sex determination by the histone demethylase Jmjd1a. *Science* **341**, 1106-1109.

Laurent, B., Ruitu, L., Murn, J., Hempel, K., Ferrao, R., Xiang, Y., Liu, S., Garcia, B. A., Wu, H., Wu, F. et al. (2015). A specific LSD1/KDM1A isoform regulates neuronal differentiation through H3K9 demethylation. *Mol. Cell* **57**, 957-970.

Lee, S.-K. and Pfaff, S. L. (2003). Synchronization of neurogenesis and motor neuron specification by direct coupling of bHLH and homeodomain transcription factors. *Neuron* **38**, 731-745.

Lee, J. E., Hollenberg, S. M., Snider, L., Turner, D. L., Lipnick, N. and Weintraub, H. (1995). Conversion of Xenopus ectoderm into neurons by NeuroD, a basic helix-loop-helix protein. *Science* **268**, 836-844.

Lee, S., Lee, B., Lee, J. W. and Lee, S.-K. (2009). Retinoid signaling and neurogenin2 function are coupled for the specification of spinal motor neurons through a chromatin modifier CBP. *Neuron* **62**, 641-654.

Liu, Z., Zhou, S., Liao, L., Chen, X., Meistrich, M. and Xu, J. (2010). Jmjd1a demethylase-regulated histone modification is essential for cAMP-response element modulator-regulated gene expression and spermatogenesis. *J. Biol. Chem.* **285**, 2758-2770.

Liu, M.-L., Zang, T., Zou, Y., Chang, J. C., Gibson, J. R., Huber, K. M. and Zhang, C. L. (2013). Small molecules enable neurogenin 2 to efficiently convert human fibroblasts into cholinergic neurons. *Nat. Commun.* **4**, 2183.

Liu, M.-L., Zang, T. and Zhang, C.-L. (2016). Direct lineage reprogramming reveals disease-specific phenotypes of motor neurons from human ALS patients. *Cell Rep.* **14**, 115-128.

Loh, Y.-H., Zhang, W., Chen, X., George, J. and Ng, H.-H. (2007). Jmjd1a and Jmjd2c histone H3 Lys 9 demethylases regulate self-renewal in embryonic stem cells. *Genes Dev.* **21**, 2545-2557.

Ma, Q., Kintner, C. and Anderson, D. J. (1996). Identification of neurogenin, a vertebrate neuronal determination gene. *Cell* **87**, 43-52.

Masserdotti, G., Gillotin, S., Sutor, B., Drechsel, D., Irmler, M., Jorgensen, H. F., Sass, S., Theis, F. J., Beckers, J., Berninger, B. et al. (2015). Transcriptional mechanisms of proneural factors and REST in regulating neuronal reprogramming of astrocytes. *Cell Stem Cell* **17**, 74-88.

Matsukawa, S., Miwata, K., Asashima, M. and Michiue, T. (2015). The requirement of histone modification by PRDM12 and Kdm4a for the development of pre-placodal ectoderm and neural crest in Xenopus. *Dev. Biol.* **399**, 164-176.

Mattar, P., Britz, O., Johannes, C., Nieto, M., Ma, L., Rebeyka, A., Klenin, N., Polleux, F., Guillemot, F. and Schuurmans, C. (2004). A screen for downstream effectors of Neurogenin2 in the embryonic neocortex. *Dev. Biol.* **273**, 373-389.
Mattar, P., Langevin, L. M., Markham, K., Klenin, N., Shivji, S., Zinyk, D. and Schuurmans, C. (2008). Basic helix-loop-helix transcription factors cooperate to specify a cortical projection neuron identity. *Mol. Cell. Biol.* **28**, 1456-1469.
Maze, I., Noh, K.-M. and Allis, C. D. (2013). Histone regulation in the CNS: basic principles of epigenetic plasticity. *Neuropsychopharmacology* **38**, 3-22.
Maze, I., Wenderski, W., Noh, K.-M., Bagot, R. C., Tzavaras, N., Purushothaman, I., Elsässer, S. J., Guo, Y., Ionete, C., Hurd, Y. L. et al. (2015). Critical role of histone turnover in neuronal transcription and plasticity. *Neuron* **87**, 77-94.
Miyata, T., Maeda, T. and Lee, J. E. (1999). NeuroD is required for differentiation of the granule cells in the cerebellum and hippocampus. *Genes Dev.* **13**, 1647-1652.
Mizuguchi, R., Sugimori, M., Takebayashi, H., Kosako, H., Nagao, M., Yoshida, S., Nabeshima, Y., Shimamura, K. and Nakafuku, M. (2001). Combinatorial roles of olig2 and neurogenin2 in the coordinated induction of pan-neuronal and subtype-specific properties of motoneurons. *Neuron* **31**, 757-771.
Moody, S. A., Miller, V., Spanos, A. and Frankfurter, A. (1996). Developmental expression of a neuron-specific beta-tubulin in frog (Xenopus laevis): a marker for growing axons during the embryonic period. *J. Comp. Neurol.* **364**, 219-230.
Novitch, B. G., Chen, A. I. and Jessell, T. M. (2001). Coordinate regulation of motor neuron subtype identity and pan-neuronal properties by the bHLH repressor Olig2. *Neuron* **31**, 773-789.
Okada, Y., Scott, G., Ray, M. K., Mishina, Y. and Zhang, Y. (2007). Histone demethylase JHDM2A is critical for Tnp1 and Prm1 transcription and spermatogenesis. *Nature* **450**, 119-123.
Ozen, I., Galichet, C., Watts, C., Parras, C., Guillemot, F. and Raineteau, O. (2007). Proliferating neuronal progenitors in the postnatal hippocampus transiently express the proneural gene Ngn2. *Eur. J. Neurosci.* **25**, 2591-2603.
Pang, Z. P., Yang, N., Vierbuchen, T., Ostermeier, A., Fuentes, D. R., Yang, T. Q., Citri, A., Sebastiano, V., Marro, S., Sudhof, T. C. et al. (2011). Induction of human neuronal cells by defined transcription factors. *Nature* **476**, 220-223.
Qi, H. H., Sarkissian, M., Hu, G.-Q., Wang, Z., Bhattacharjee, A., Gordon, D. B., Gonzales, M., Lan, F., Ongusaha, P. P., Huarte, M. et al. (2010). Histone H4K20/H3K9 demethylase PHF8 regulates zebrafish brain and craniofacial development. *Nature* **466**, 503-507.
Quan, X.-J., Yuan, L., Tiberi, L., Claeys, A., De Geest, N., Yan, J., van der Kant, R., Xie, W. R., Klisch, T. J., Shymkowitz, J. et al. (2016). Post-translational control of the temporal dynamics of transcription factor activity regulates neurogenesis. *Cell* **164**, 460-475.
Raposo, A. A., Vasconcelos, F. F., Drechsel, D., Marie, C., Johnston, C., Dolle, D., Bithell, A., Gillotin, S., van den Berg, D. L. C., Ettwiller, L. et al. (2015). Ascl1 coordinately regulates gene expression and the chromatin landscape during neurogenesis. *Cell Rep.* **10**, 1544-1556.
Sasai, Y., Lu, B., Steinbeisser, H., Geissert, D., Gont, L. K. and De Robertis, E. M. (1994). Xenopus chordin: a novel dorsalizing factor activated by organizer-specific homeobox genes. *Cell* **79**, 779-790.
Seo, S., Richardson, G. A. and Kroll, K. L. (2005). The SWI/SNF chromatin remodeling protein Brg1 is required for vertebrate neurogenesis and mediates transactivation of Ngn and NeuroD. *Development* **132**, 105-115.
Seo, S., Lim, J.-W., Yellajoshyula, D., Chang, L.-W. and Kroll, K. L. (2007). Neurogenin and NeuroD direct transcriptional targets and their regulatory enhancers. *EMBO J.* **26**, 5093-5108.
Simmons, A. D., Horton, S., Abney, A. L. and Johnson, J. E. (2001). Neurogenin2 expression in ventral and dorsal spinal neural tube progenitor cells is regulated by distinct enhancers. *Dev. Biol.* **229**, 327-339.
Sive, H., Grainger, R. and Harland, R. M. (2000). *Early Development Xenopus laevis*: A Laboratory Manual. Cold Spring Harbor, New York: Cold Spring Harbor Laboratory Press.
Smallwood, A., Esteve, P.-O., Pradhan, S. and Carey, M. (2007). Functional cooperation between HP1 and DNMT1 mediates gene silencing. *Genes Dev.* **21**, 1169-1178.
Smith, W. C. and Harland, R. M. (1992). Expression cloning of noggin, a new dorsalizing factor localized to the Spemann organizer in Xenopus embryos. *Cell* **70**, 829-840.
Snowden, A. W., Gregory, P. D., Case, C. C. and Pabo, C. O. (2002). Gene-specific targeting of H3K9 methylation is sufficient for initiating repression in vivo. *Curr. Biol.* **12**, 2159-2166.
Sommer, L., Ma, Q. and Anderson, D. J. (1996). Neurogenins, a novel family of atonal-related bHLH transcription factors, are putative mammalian neuronal determination genes that reveal progenitor cell heterogeneity in the developing CNS and PNS. *Mol. Cell. Neurosci.* **8**, 221-241.
Soshnev, A. A., Josefowicz, S. Z. and Allis, C. D. (2016). Greater than the sum of parts: complexity of the dynamic epigenome. *Mol. Cell* **62**, 681-694.
Strobl-Mazzulla, P. H., Sauka-Spengler, T. and Bronner-Fraser, M. (2010). Histone demethylase JmjD2A regulates neural crest specification. *Dev. Cell* **19**, 460-468.
Talikka, M., Perez, S. E. and Zimmerman, K. (2002). Distinct patterns of downstream target activation are specified by the helix-loop-helix domain of proneural basic helix-loop-helix transcription factors. *Dev. Biol.* **247**, 137-148.
Tateishi, K., Okada, Y., Kallin, E. M. and Zhang, Y. (2009). Role of Jhdm2a in regulating metabolic gene expression and obesity resistance. *Nature* **458**, 757-761.
Thoma, E. C., Wischmeyer, E., Offen, N., Maurus, K., Sirén, A.-L., Schartl, M. and Wagner, T. U. (2012). Ectopic expression of neurogenin 2 alone is sufficient to induce differentiation of embryonic stem cells into mature neurons. *PLoS ONE* **7**, e38651.
Thuret, R., Auger, H. and Papalopulu, N. (2015). Analysis of neural progenitors from embryogenesis to juvenile adult in Xenopus laevis reveals biphasic neurogenesis and continuous lengthening of the cell cycle. *Biol. Open* **4**, 1772-1781.
Tien, C.-L., Jones, A., Wang, H., Gerigk, M., Nozell, S. and Chang, C. (2015). Snail2/Slug cooperates with Polycomb repressive complex 2 (PRC2) to regulate neural crest development. *Development* **142**, 722-731.
Tsukada, Y.-I., Ishitani, T. and Nakayama, K. I. (2010). KDM7 is a dual demethylase for histone H3 Lys 9 and Lys 27 and functions in brain development. *Genes Dev.* **24**, 432-437.
Vasconcelos, F. F., Sessa, A., Laranjeira, C., Raposo, A. A., Teixeira, V., Hagey, D. W., Tomaz, D. M., Muhr, J., Broccoli, V. and Castro, D. S. (2016). MyT1 counteracts the neural progenitor program to promote vertebrate neurogenesis. *Cell Rep.* **17**, 469-483.
Vierbuchen, T. and Wernig, M. (2012). Molecular roadblocks for cellular reprogramming. *Mol. Cell* **47**, 827-838.
Vierbuchen, T., Ostermeier, A., Pang, Z. P., Kokubu, Y., Südhof, T. C. and Wernig, M. (2010). Direct conversion of fibroblasts to functional neurons by defined factors. *Nature* **463**, 1035-1041.
Wang, J., Park, J. W., Drissi, H., Wang, X. and Xu, R.-H. (2014a). Epigenetic regulation of miR-302 by JMJD1C inhibits neural differentiation of human embryonic stem cells. *J. Biol. Chem.* **289**, 2384-2395.
Wang, W.-L., Anderson, L. C., Nicklay, J. J., Chen, H., Gamble, M. J., Shabanowitz, J., Hunt, D. F. and Shechter, D. (2014b). Phosphorylation and arginine methylation mark histone H2A prior to deposition during Xenopus laevis development. *Epigenet. Chromatin* **7**, 22.
Wapinski, O. L., Vierbuchen, T., Qu, K., Lee, Q. Y., Chanda, S., Fuentes, D. R., Giresi, P. G., Ng, Y. H., Marro, S., Neff, N. F. et al. (2013). Hierarchical mechanisms for direct reprogramming of fibroblasts to neurons. *Cell* **155**, 621-635.
Wilkinson, G., Dennis, D. and Schuurmans, C. (2013). Proneural genes in neocortical development. *Neuroscience* **253**, 256-273.
Xanthos, J. B., Kofron, M., Tao, Q., Schaible, K., Wylie, C. and Heasman, J. (2002). The roles of three signaling pathways in the formaiton and function of the Spemann Organizer. *Development* **129**, 4027-4043.
Yamane, K., Toumazou, C., Tsukada, Y., Erdjument-Bromage, H., Tempst, P., Wong, J. and Zhang, Y. (2006). JHDM2A, a JmjC-containing H3K9 demethylase, facilitates transcription activation by androgen receptor. *Cell* **125**, 483-495.
Yang, N., Ng, Y. H., Pang, Z. P., Südhof, T. C. and Wernig, M. (2011). Induced neuronal cells: how to make and define a neuron. *Cell Stem Cell* **9**, 517-525.
Zhang, Y., Ding, Y., Chen, Y.-G. and Tao, Q. (2014). NEDD4L regulates convergent extension movements in Xenopus embryos via Disheveled-mediated non-canonical Wnt signaling. *Dev. Biol.* **392**, 15-25.

Supplementary Materials

Extended Materials and Methods

1. ChIP-qPCR.

ChIP experiments were performed through procedure as described in (Shelby A. Blythe 2009) with minor modifications. Briefly, 50 embryos at the desired stages were fixed in 1% formaldehyde for 10 minutes at room temperature followed by washing in 0.125 M glycine for 10 minutes. After washing 3 times in pre-cold PBS, embryos can be stored at -80 degree. RIPA buffer (10 mM Tris-HCl pH 8.0, 1 mM EDTA, 140 mM NaCl, 1% Triton X-100, 0.2% SDS, 0.1% Sodium Deoxycholate) was used to homogenize the fixed embryos followed by incubating embryos on ice for at least 10 min. After centrifugation, supernatant was discarded and the pellet was resuspended in RIPA buffer. Sonication was performed by 24 cycles with 2s on and 3s off. After centrifugation, the supernatant was pre-cleared using 10 µl blocked Dynabeads protein A (Life Tech, #10001D, Massachusetts, USA) or Dynabeads protein G (Life Tech, #10003D). Blocking buffer was 0.5% BSA, 0.5% Tween20 in PBS. After blocking, the supernatant was diluted 3 times using SDS-free RIPA buffer. 1% diluted supernatant was stored as input. 1 µg antibody (αMyc, αKDM3A, αH3K9me2, αH3K4me3, αH3K27ac, see detailed information for antibodies in the supplementary Table S2) or normal IgG was used for immunoprecipitation at 4 degree overnight. 20 µl blocked Dynabeads were used to pull down antibodies for at least 3 hours. Dynabeads were then washed by Buffer I

(20 mM Tris-HCl pH8.0, 0.1% SDS, 1% Triton X-100, 2mM EDTA, 150 mM NaCl), Buffer II (20 mM Tris-HCl pH8.0, 0.1% SDS, 1% Triton X-100, 2mM EDTA, 500 mM NaCl), Buffer III (10 mM Tris pH8.0, 0.25 M LiCl, 1% NP-40, 1% Na-Deoxycholate, 1 mM EDTA), TE Buffer (10 mM Tris-HCl pH 8.0, 1 mM EDTA). Use 2 washes with each and every buffer. TES Buffer (50 mM Tris-HCl pH8.0, 10 mM EDTA, 1% SDS) was used to incubate Dynabeads for 20 min at 65 degree. Then Proteinase K was added to reverse crosslinks and digest proteins at 65 degree overnight. ChIP DNA was purified using phenol-chloroform and resuspended in TE buffer. Then the qPCR programs were performed using an FQD-96A^{TM} machine (BIOER, Hangzhou China).

2. ***Neuron induction and Co-immunoprecipitation (CoIP)***

Mouse neuronal cells were obtained by treating NE-4C cells with 1 □M all-trans retinoic acid (Schlett and Madarasz, 1997). Human neuronal cells were generated from primitive neural stem cells derived from H9 human stem cell line, following established protocol as described (Yan et al., 2013).

For immunoprecipitation analysis, cells from one well of 6-well plate were lysed with TNE buffer (10 mM Tris pH 7.4, 150 mM NaCl, 0.5% NP-40, 1 mM EDTA) containing proteinase inhibitor cocktail (Roche), and 40% of the total lysate was used for immunoprecipitation with 0.5 □g of anti-KDM3A (Abcam) and anti-Ngn2 (Santa Cruz Biotechnology) antibodies, with 1.5 mg of Dynableads A (Novex, Life Technology) as instructed. A quarter of the eluted antigen product was subjected to

western blotting with anti-KDM3A and anti-Neurog2 antibodies. As input control, 12.5 μg of protein lysate was also loaded.

3. Dual-luciferase reporter assay

Dual-luciferase reporter assay was performed using Promega luciferase system (E1960, Promega, Wisconsin, USA) following procedures provided in the manufacture's manual. Briefly, 20 pg wild type or mutant tubb2b promoter plasmid (subcloned into pGL3-basic at MluI/XhoI sites) and 10 pg Renilla plasmid were injected into animal pole of 4-cell stage embryos with/without 100 pg *neurog2* or β-*gal* mRNA. Embryos were collected at stage 14/15. Each treatment group was sampled as triplicates. 30 counts of embryos were collected for each sample. Embryo samples were then lysed using 450 □l Passive Lysis Buffer. After centrifugation, supernatant was collected for dual-luciferase test using a Synergy H1 Hybrid Reader (BioTek, Winooski, USA). Data presented in the supplementary figure S6B represent mean +/- SEM (standard error of mean) from three independent experiments.

References:

Schlett, K. and Madarasz, E. 1997. Retinoic acid induced neural differentiation in a neuroectodermal cell line immortalized by p53 deficiency. J Neurosci Res 47(4): 405-15.

Yan, Y., Shin, S., Jha, B. S., Liu, Q., Sheng, J., Li, F., Zhan, M., Davis, J., Bharti, K., Zeng, X. et al. 2013. Efficient and rapid derivation of primitive neural stem cells and generation of brain subtype neurons from human pluripotent stem cells. Stem Cells Transl Med 2(11): 862-70.

Supplementary Tables

Supplementary Table S1: in situ probe constructs used in this study.

In Situ Probe		
Items	**Linearization Enzymes**	**Vectors**
Kdm3a	BglII/T7	pCS107
Sox2	HindIII/T7	pCS107
Otx2	NotI/T7	pCS107
Rx	ClaI/T7	pCS107
Pax6	BamHI/T7	pCS107
Six3	ClaI/T7	pCS107
Sox3	BamHI/T7	pCS107
Xk81b2	HindIII/T7	pCS107
Msx1	EcoRI/T7	pCS107
Zic1	EcoRI/T7	pCS107
Sox9	ClaI/T7	pCS107
Snail1	ClaI/T7	pCS107
En2	XbaI/T3	pBSKS
Krox20	BamHI/T7	pCS107
Hoxb9	XbaI/T3	pBSKS
Ath5	ClaI/T7	pCS107
Neurog2	BamHI/T7	pCS107
Ascl1	BamHI/T7	pCS107
Neurod1	ClaI/T7	pCS107
Tubb2b	BamHI/T7	pCS107
Dll1	EcoRV/T7	pCS2
Runx1	ClaI/T7	pCS107
HB9	EcoRI/T7	pCS107
xHox11L2	EcoRI/T7	pCS107

Supplementary Table S2: antibodies used in this study

Antibody		
Antibody	**Supplier**	**Cat.#**
Anti-H3	Cell signaling	9715
Anti-H3K9me1	Millipore	07-450
Anti-H3K9me2	Abcam	ab1220
Anti-H3K9me3	Millipore	07-523
Anti-H3K9ac	millipore	06-942
Anti-H3K27ac	millipore	07-360
Anti-H3K27me3	millipore	ABE44
Anti-H3K4me3	millipore	07-473
Anti-Kdm3A	Abcam	ab80598
Anti-Kdm4A	Abcam	ab70786
Anti-Myc	Santa Cruz	sc-40
Anti-Flag	Sigma	F1804
Anti-HA	Roche	11867423001
Anti-Neurog2	Santa Cruz	sc-19233
Anti-phospho-Erk1/2(Thr-202/Tyr204)	Cell signaling	9101
Anti-Erk1/2(p44/42 MAPK)	Cell signaling	9102

Supplementary Table S3: oligos and primers used in this study

Click here to Download Table S3

Supplementary Table S4: KDM3A MS qPCR raw data

Click here to Download Table S4

Supplementary Figure

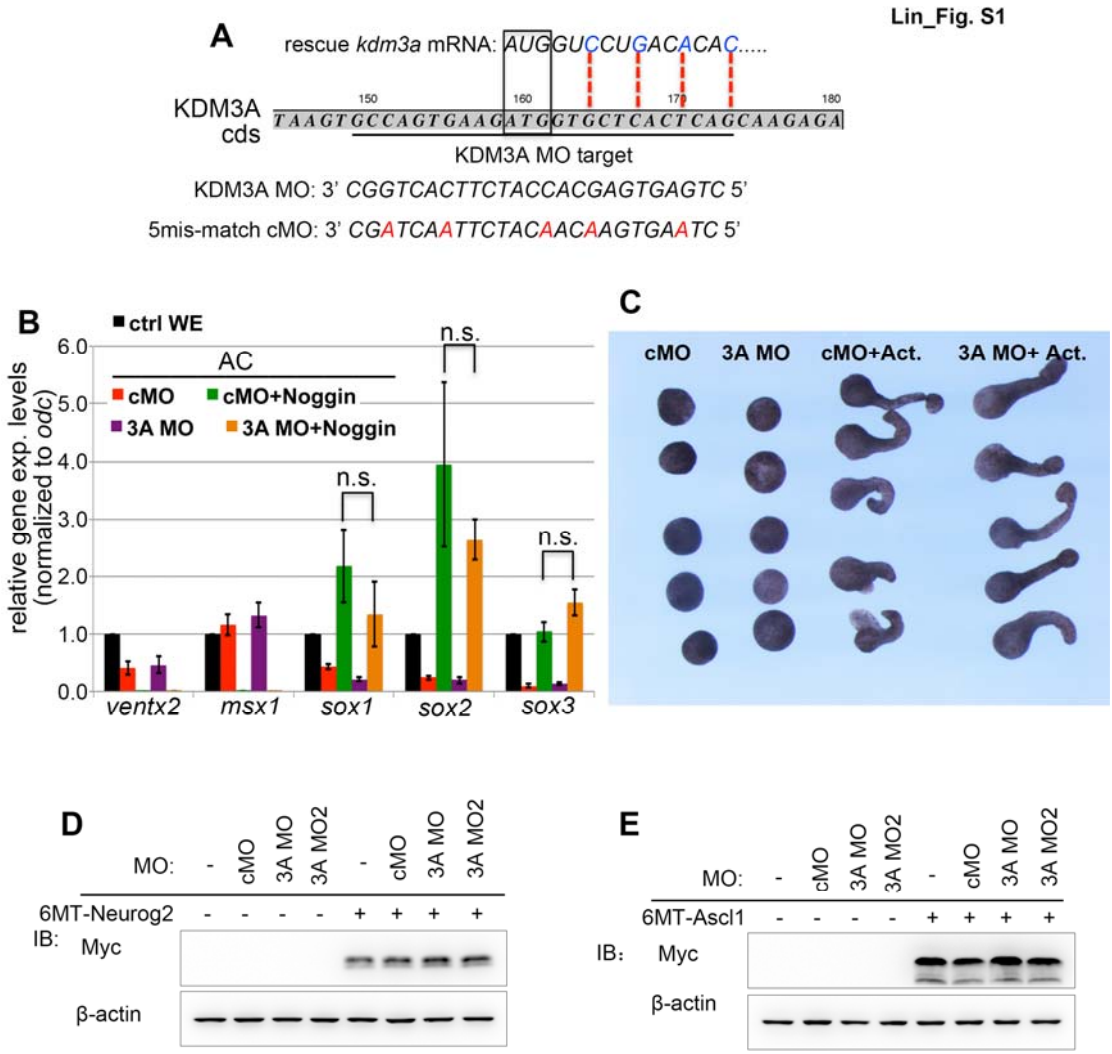

Fig. S1 (related to Fig. 1). MO-mediated depletion of KDM3A and assessment of the function of KDM3A in the developmental potential of naïve ectoderm.

(A) Schematic depiction of the start codon spanning sequence of KDM3A CDS and the KDM3A MO target sequence. The sequence of a 5mis-match mutant version of KDM3A MO, designed cMO, shown in comparison with the KDM3A MO. (B) qPCR analyses of gene expression in animal cap explants. cMO: 80ng; 3A MO: 80ng.

Noggin mRNA: 200 pg. WE: whole embryo; AC: animal cap explants. ns: no significance according to two-tailed Student *t*-test. (C) Animal cap explants treated with or without Activin protein. 80ng cMO and 3A MO were injected into the animal pole at the 2-cellstage and animal caps were dissected at the stage 8.5 and treated with or without Activin (5 ng/ml) for four hours. All explants were then cultured in simple saline to the sibling stage 18. (D, E) Western blot data showing that KDM3A MO/MO2 injection did not affect the expression of microinjected 6MT-Neurog2 (D) or 6MT-Ascl1 (E). cMO: 80 ng; 3A MO: 80 ng; 3A MO2: 80 ng. 6MT-*neurog2* mRNA: 500 pg; MT-*ascl1*: 200 pg. MO and mRNA were sequentially injected into both cells at the 2-cell stage. Embryos were lysed at stage 11.

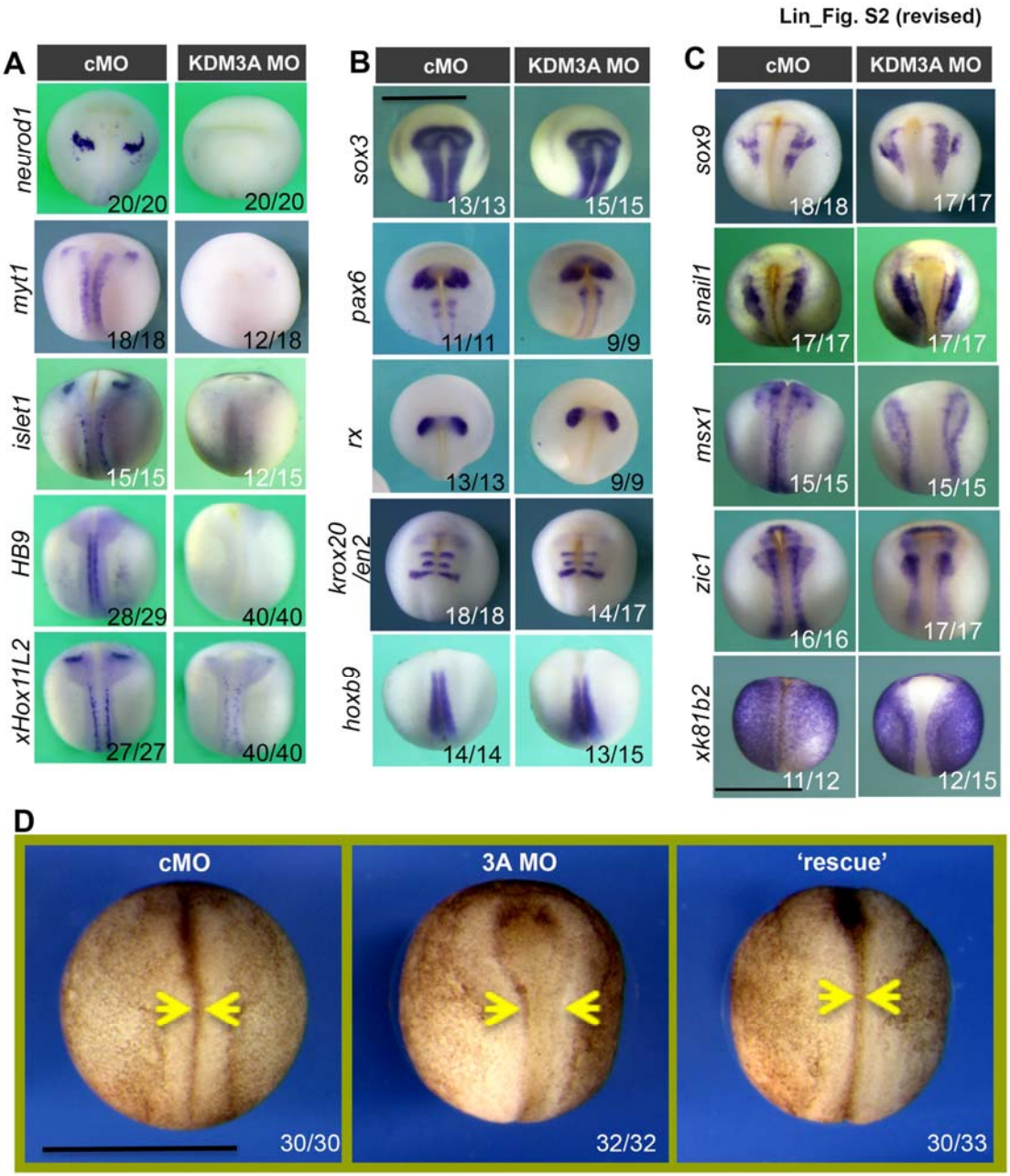

Fig. S2 (related to Fig. 2). Assessment of the effects of KDM3A depletion on neural development.

(A, B, C) Control (cMO) and KDM3A morphant (3A MO) embryos at stage 18*in situ* hybridized with indicated marker genes. (A) Neuronal genes. (B) Markers for neural

progenitors (*sox3, pax6*) and the anteroposterior pattern (*rx*, *krox20*, *en2*, and *hoxb9*). (C) Markers for neural plate border, neural crest specification and epidermis. (D) Dorsal view of embryos at stage 18 showing that KDM3A depletion by injecting 60 ng 3A MO delays neural tube closure, which was partially rescued by injecting back of 500 pg the MO-resistant *kdm3a* mRNA.

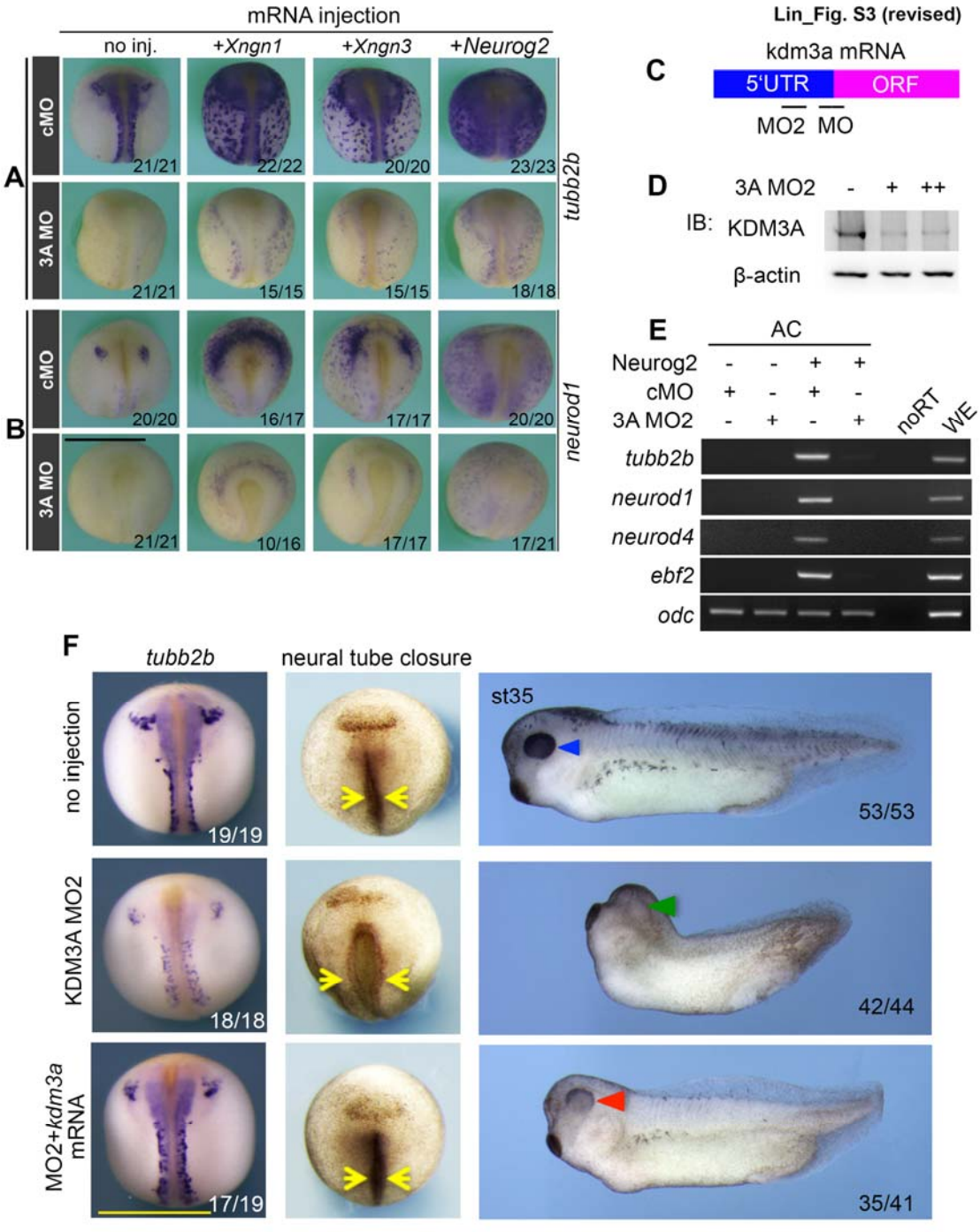

Fig. S3 (related to Fig. 2). KDM3A is required for primary neurogenesis in *Xenopus* and depletion of KDM3A using a second MO (MO2). (A, B) Embryos at stage 18 in situ hybridized with *tubb2b* (A, dorsal view) or *neurod1* (B, dorsal anterior view). 80 ng 3A MO or cMO was injected into both cells at the 2-cell stage. mRNA encoding Xneurog1 (100 pg), Xneurog3 (100 pg), or mouse Neurog2 (50 pg) was injected into two dorsal cells at the 4-cell stage. (C) A schematic depiction of KDM3A MO and MO2 targeting different locations that are critical for the translation control of *kdm3a* mRNA. (D) Western blot detection of KDM3A protein at stage 11 after KDM3A MO2 injection at the 2-cell stage (40 and 80 ng). (E) Semi-quantitative PCR analyses of gene expression in animal caps with indicated treatment. cMO: 80 ng. 3A MO2: 80 ng. *neurog2* mRNA: 100 pg. (F) Effects of KDM3A MO2 injection on *tubb2b* expression analyzed through WISH (left column, dorsal view), neural tube closure (middle column, dorsal anterior view, yellow arrows demarcate the closing neural tubes), and later development (right column, lateral view, solid triangles indicate eyes). cMO: 60 ng. 3A MO2: 60 ng. 3A MO2-resistant *kdm3a* mRNA: 500 pg.

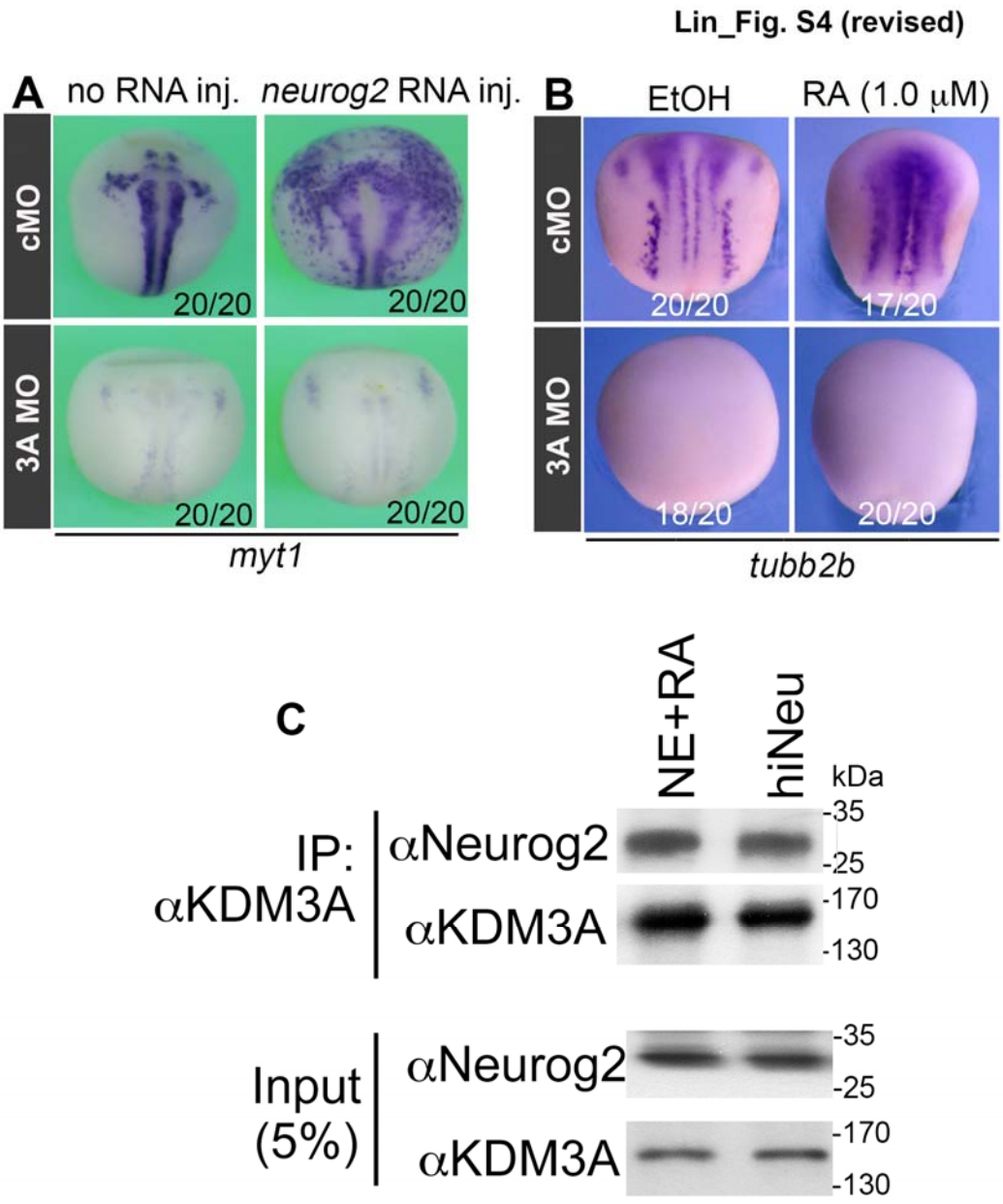

Fig. S4 (related to Figs. 3 and 4). Assessment of functional and physical interactions between KDM3A and Neurog2.

(A) WISH detection of *myt1* in embryos at stage 18 (dorsal view). cMO and 3A MO: 80 ng. *neurog2* mRNA:100 pg. (B) Embryos at stage 15/16 in situ hybridized with

tubb2b (dorsal view). 3A MO and cMO: 80 ng. RA (1.0 μM) was added to culture medium from stage 12 to stage 15/16. (C) Two different types of cells (RA-induced NE-4C cells and human induced-Neu neural stem cells) were lysed and subjected to CoIP for detecting interaction between the endogenous KDM3A and Neurog2. A KDM3A antibody was used to pull down endogenous KDM3A protein, and a Neurog2 antibody was used to detect the signal of endogenous Neurog2 protein.

Lin_Fig. S5 (revised)

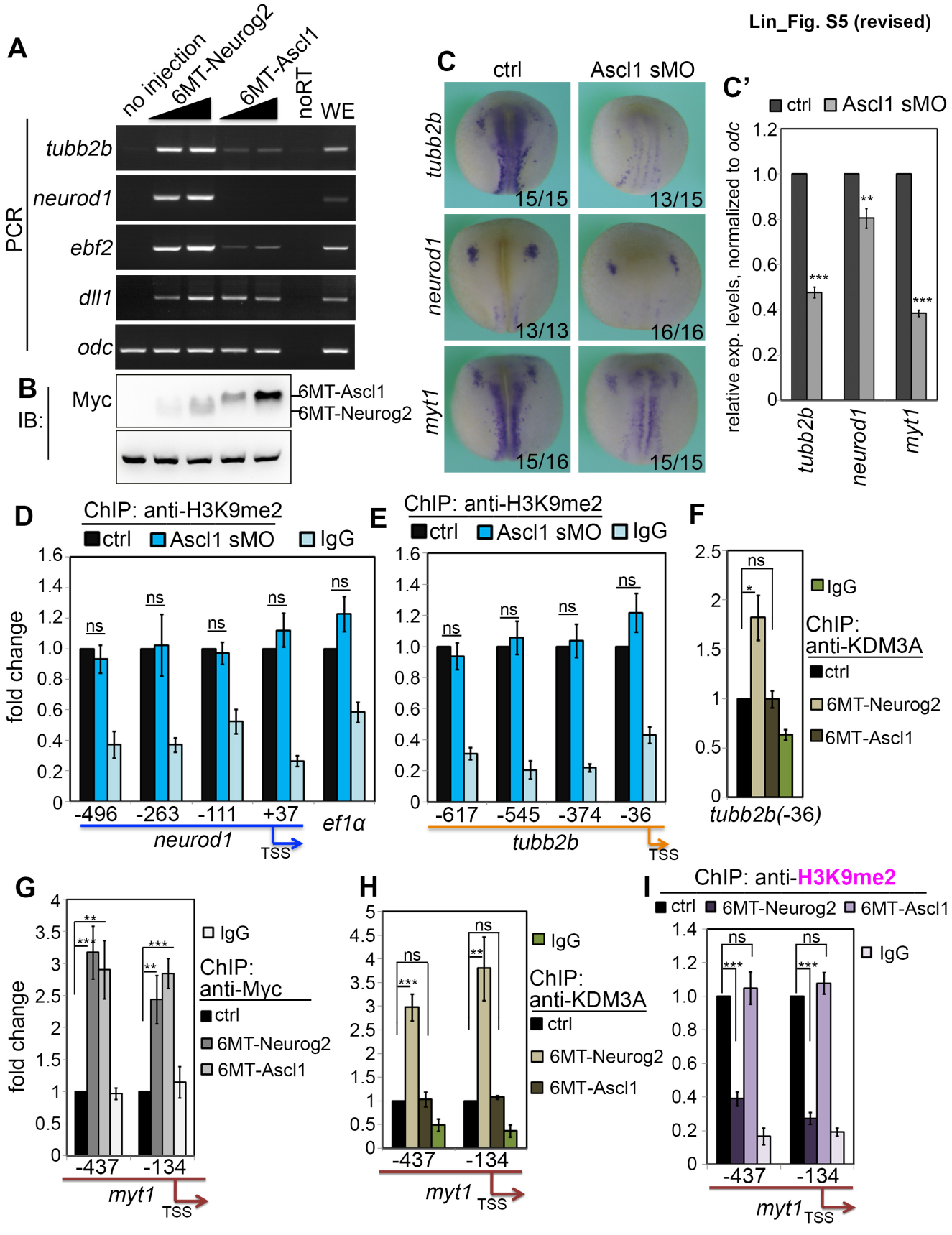

Fig. S5 (related to Fig. 5). Assessment of the activities of Ascl1 on neuronal gene expression and H3K9me2.

(A) Semi-quantitative PCR analyses of gene expression in animal cap explants treated with Neurog2 or Ascl1. (B) Western blot detection of overexpressed 6MT-Neurog2 and 6MT-Ascl1 in the animal cap explants prepared through the same procedure as done in (A). (C, C') WISH (C) and RT-qPCR (C') detection of gene expression in control and Ascl1 splice blocking MO (Ascl1 sMO, 80 ng)-injected embryos at the stage 18. * P<0.05; ** P<0.01; *** P<0.005, according to two-tailed Student t-test.. (D, E) Anti-H3K9me2 ChIP-qPCR analyses showing that 80 ng Ascl1 sMO did not alter the H3K9me2 marks on the promoter regions of *neurod1* (D) or *tubb2b* (E). (F) ChIP-qPCR detection of KDM3A on the -36 bp position of *tubb2b* promoter. 6MT-*neurog2* mRNA (500 pg) and 6MT-*ascl1* mRNA (200 pg) were individually injected at the 2-cell stage and embryos were then harvested at the stage 15 followed by ChIP-qPCR procedures. (G-I) ChIP-qPCR data showing the effects of ectopic Neurog2 and Ascl1 on the promoter region of *myt1*. Both ectopic Neurog2 and Ascl1 were able to bind *myt1* promoter (G). Only overexpressed Neurog2 increased the level of KDM3A (H), and decreased the H3K9me2 marks (I) on the promoter of *myt1*. * P<0.05; ** P<0.01; *** P<0.005; ns: no significance, according to two-tailed Student's t-test.

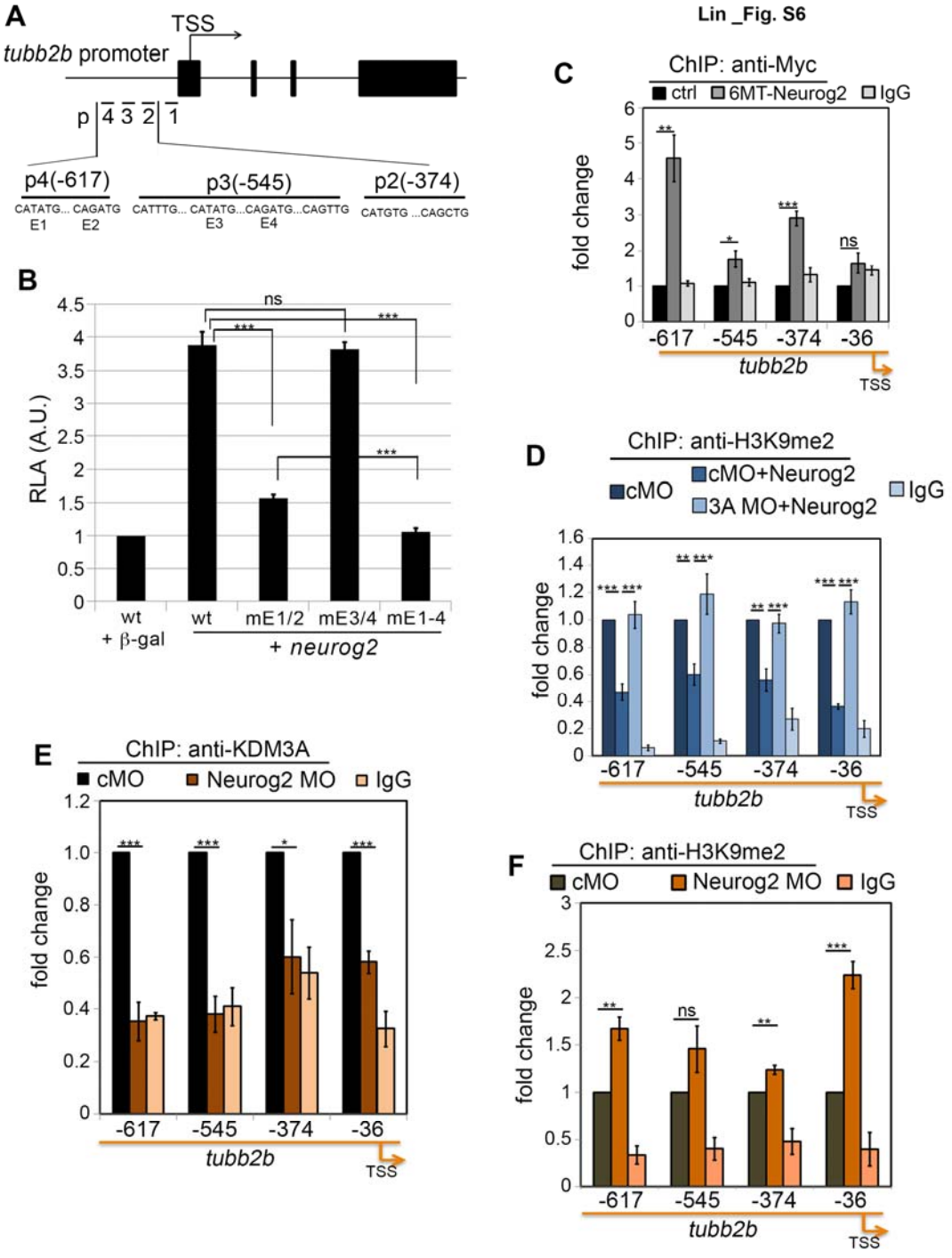

Fig. S6 (related to Fig. 5). Neurog2 transactivates *tubb2b* in a KDM3A-dependent manner.

(A) Schematics of the *tubb2b* promoter and upstream regulatory sequences that contain several degenerate E-box motifs. Locations of ChIP-qPCR primers are also shown. (B) Dual-luciferase reporter assays showing that the *tubb2b* promoter-driven luciferase reporter is responsive to overexpressed 100 pg *neurog2* depending the presence of intact E-box motifs (E1 and E2). (C) ChIP-qPCR analysis of the binding of overexpressed 6MT-Neurog2 on the promoter region of *tubb2b*. (D) Anti-H3K9me2 ChIP-qPCR analyses showing that 80 ng 3A MO abolished the ability of ectopic Neurog2 (100 pg) to decrease theH3K9me2 marks on the *tubb2b* promoter. (E) Anti-KDM3A ChIP-qPCR analyses at stage 15 indicating that Neurog2 MO (80 ng) but not standard MO reduced KDM3A bound on the *tubb2b* promoter. (F) Anti-H3K9me2 ChIP-qPCR at stage 18 showing that Neurog2 (80 ng) but not control MO increased the H3K9me2 marks on the *tubb2b* promoter. * $P<0.05$; ** $P<0.01$; ***$P<0.005$, ns: no significance, according to two-tailed Student's *t*-test.

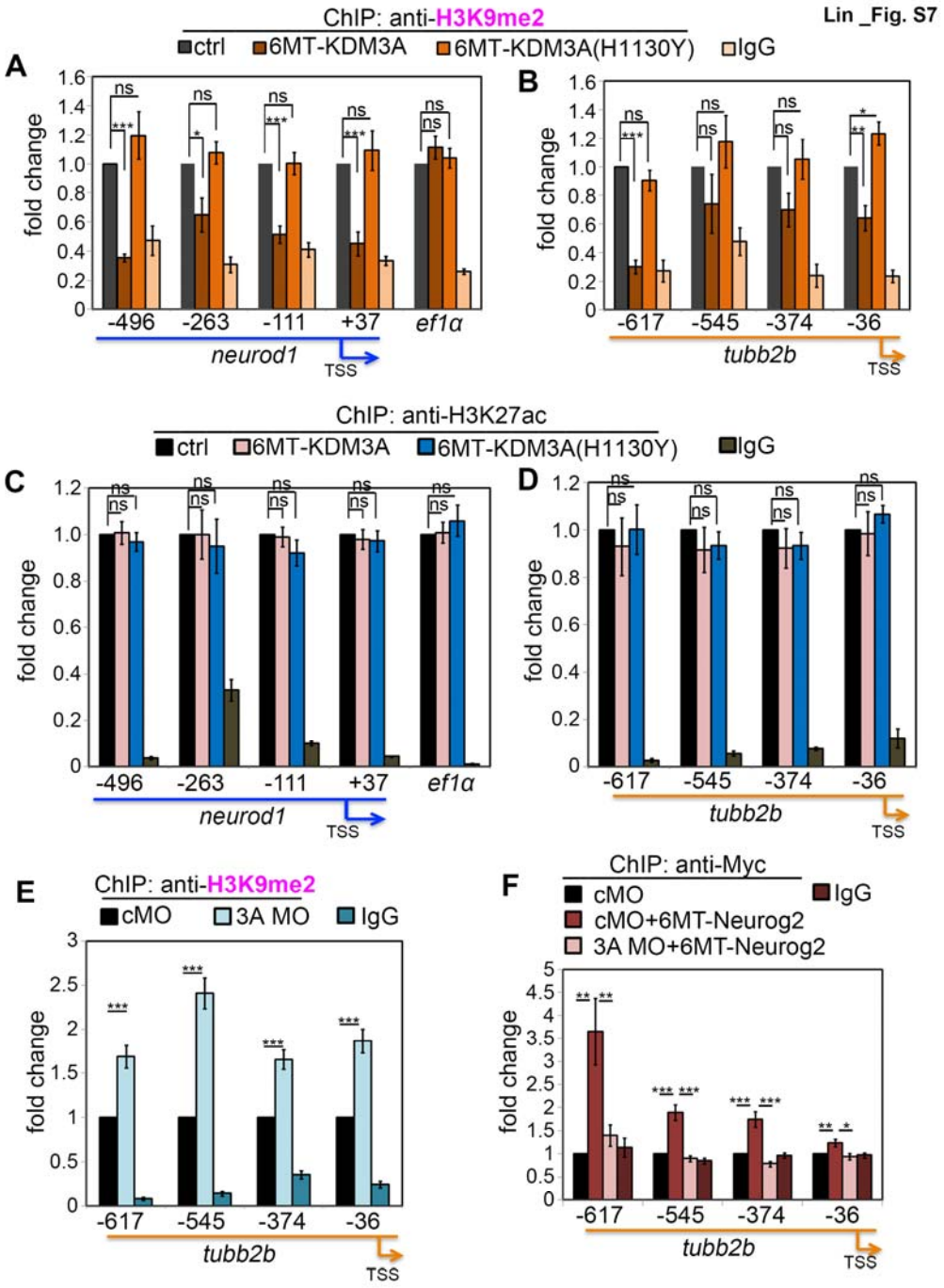

Fig.S7 (related to Figs. 5 and 6). KDM3A facilitates the chromatin binding of Neurog2.

(A, B) Anti-H3K9me2 ChIP-qPCR analyses indicating that overexpression of wild type 6MT-KDM3A (1 ng) but not a catalytic mutant 6MT-KDM3A (H1130Y, 1 ng) reduced the expression levels of H3K9me2 on the promoter regions of *neurod1* (A) and *tubb2b* (B). (C, D) Anti-H3K27ac ChIP-qPCR analyses indicating that ectopic 6MT-KDM3A or a catalytic mutant 6MT-KDM3A (H1130Y) did not alter the H3K27ac marks on the promoter regions of *neurod1* (C) or *tubb2b* (D). (E) Anti-H3K9me2ChIP-qPCR analyses showing 3A MO (80 ng) increased the H3K9me2 marks on the promoter region of *tubb2b*. (F) Anti-Myc ChIP-qPCR analyses indicating that 80 ng 3A MO but not cMO blocked the overexpressed 6MT-Neurog2 from accessing the promoter of *tubb2b*.